Nanoscale

REVIEW

View Article Online
View Journal | View Issue

Cite this: *Nanoscale*, 2023, **15**, 18550

Light-driven micro/nanomotors in biomedical applications

Xuejiao Zeng,†[a,b,c] Mingzhu Yang,†[a,b,c] Hua Liu,†[a,b,c] Zhenzhong Zhang,[a,b,c,d] Yurong Hu,* [a,b,c,d] Jinjin Shi* [a,b,c,d] and Zhi-Hao Wang* [a,b,c,d]

Nanotechnology brings hope for targeted drug delivery. However, most current drug delivery systems use passive delivery strategies with limited therapeutic efficiency. Over the past two decades, research on micro/nanomotors (MNMs) has flourished in the biomedical field. Compared with other driven methods, light-driven MNMs have the advantages of being reversible, simple to control, clean, and efficient. Under light irradiation, the MNMs can overcome several barriers in the body and show great potential in the treatment of various diseases, such as tumors, and gastrointestinal, cardiovascular and cerebrovascular diseases. Herein, the classification and mechanism of light-driven MNMs are introduced briefly. Subsequently, the applications of light-driven MNMs in overcoming physiological and pathological barriers in the past five years are highlighted. Finally, the future prospects and challenges of light-driven MNMs are discussed as well. This review will provide inspiration and direction for light-driven MNMs to overcome biological barriers *in vivo* and promote the clinical application of light-driven MNMs in the biomedical field.

Received 31st July 2023,
Accepted 27th October 2023

DOI: 10.1039/d3nr03760f

rsc.li/nanoscale

1. Introduction

In the past few decades, nanotechnology has developed rapidly and achieved excellent results in many fields. Currently, there is a growing interest in nanotechnology and its application in biomedical fields, especially medical diagnosis,[1] therapeutics,[2] and biomedical tools.[3] With the unremitting efforts of researchers, various drug delivery systems have emerged with improved drug activity, reduced side effects, and enhanced biological barrier penetration ability *in vivo* and *in vitro*.[4,5] For example, liposomes, polymer micro-nanoparticles, *etc.*, have been widely used in targeted drug delivery.[6,7] The so-called passive targeted delivery systems use the passive diffusion mechanism to enhance permeability and retention (EPR) effects to accumulate drugs in specific tissues.[8,9] However, EPR effects have been reported to be limited by heterogeneity and related physiological barriers,[10,11] with less than 0.7% of intravenously injected nanoparticles reaching solid tumor sites.[12] This indicates that the traditional passive targeted delivery of nanomaterials is challenging to achieve adequate transportation and tissue penetration of goods. Therefore, it is of great significance to develop a new generation of drug delivery vectors that can be remotely controlled and allow directional navigation and controllable search for specific tissue sites.

Encouragingly, micro/nanomotors (MNMs) have evolved rapidly over the past few years and have shown great promise for biomedical applications.[13] MNMs are micro–nano devices that autonomously move in a medium and cleverly utilize other forms of energy around them to convert them into mechanical motion or driving force.[14,15] MNMs have unique active movement capabilities and powerful advantages over passive diffusion, which provides the possibility to overcome the limitations of traditional passive drug delivery systems to treat a variety of diseases.[10,15] In recent years, with the in-depth exploration of nanomotors, a variety of micro–nanomotors have emerged.[16,17] In general, MNMs are classified according to the driving mechanism.[18] There are three main types of MNMs: bio-propelled MNMs, chemically propelled MNMs, and external-field propelled MNMs, each of which has its own traits in biomedical applications,[19,20] such as drug delivery,[21,22] biosensing,[23] bioimaging,[24] cancer therapy,[25,26] precision micro-/nanosurgery,[27] *etc.* Inspired by the phenomenon that a variety of cells and microorganisms in nature have autonomous movement,[28,29] scientists designed bio-propelled MNMs. However, due to the particularity of biomaterials, it is

[a]*School of Pharmaceutical Sciences, Zhengzhou University, Zhengzhou, 450001, China. E-mail: huyr@zzu.edu.cn, shijinyxy@zzu.edu.cn, wangzhihao@zzu.edu.cn*
[b]*Henan Key Laboratory of Targeting Therapy and Diagnosis for Critical Diseases, Zhengzhou, 450001, China*
[c]*Key Laboratory of Advanced Drug Preparation Technologies, Ministry of Education, Zhengzhou, 450001, China*
[d]*State Key Laboratory of Esophageal Cancer Prevention & Treatment, Zhengzhou, 450001, China*
†These authors contributed equally to this work.

difficult to apply bio-driven MNMs universally. More widely used chemically propelled MNMs can obtain driving forces from specific catalytic or spontaneous reactions in a fluid using local chemicals.[30] This requires the corresponding substrate as fuel, such as hydrogen peroxide (H_2O_2),[31–33] glucose,[34–36] urea,[37–39] and other chemicals,[40] to provide adequate energy.[41,42] External field-driven MNMs (physically driven MNMs) can respond to external physical stimulus energy and convert it into mechanical power, which is a stable and controllable energy source to avoid the side effects of chemical fuels on biological systems.[43] The exploration of external field-driven MNMs mainly focuses on light-driven MNMs,[44–46] magnetically-driven MNMs,[47–49] ultrasound-driven MNMs,[50–52] and electrically-driven MNMs.[53–55]

In particular, light-driven micro/nano devices hold great promise in precision medicine due to their reversible, simple to control, clean, and efficient properties. Light, especially sunlight, is the major energy source that powers our world and lives. With outstanding merits including abundance, remote propagation, clean energy input, and nice controllability, light has been acknowledged as a promising energy source for driving MNMs.[56] As a control signal, light promises to manipulate MNMs by modulating the light intensity, frequency, polarization, and propagation direction with spatial and temporal precision, which enables excellent controllability and programmability of light-driven MNMs.[57] Compared with other MNMs, light-driven MNMs provide energy through incident photons instead of chemically active substances, so the use of highly active but toxic chemical fuels can be avoided, indicating their better biocompatibility.[58] The light-driven mode has a high spatial and temporal resolution, which is more accurate for the control of MNMs' behavior. Furthermore, light is a suitable external stimulant to trigger MNMs' propulsion, avoiding the use of sophisticated set-ups as required by magnetic and ultrasound MNMs.[59]

Herein, the classification and mechanism of light-driven MNMs are introduced briefly, and based on the unique advantages of light-driven MNMs, this review summarized the application of light-driven nanomotors in biomedicine in the past five years. On the one hand, light-driven MNMs can be used to overcome innate barriers (*e.g.*, mucus barrier,[60] blood–brain barrier,[61] blood barrier,[62] and skin barrier[63]). On the other hand, light-driven MNMs have also been used to combat disease matrix barriers. It mainly involves deep penetration of tumor tissues,[64,65] targeted penetration into atherosclerotic plaque sites,[66] across bacterial biofilms,[67] *etc.*, to play excellent biomedical functions. Finally, the development prospects and limiting factors of MNMs were summarized to lay the foundation for the clinical application of MNMs.

2. Classification and mechanism of light-driven MNMs

Light-driven MNMs are micro/nano devices that can convert light energy into mechanical work and are able to generate driving force through asymmetric fields.[68] As an external stimulus, light has the advantages of precise control, simple operation, cleanliness and efficiency.[69] The movement of MNMs can be remotely regulated by light and their speed can also be controlled by adjusting the light intensity. Unlike chemically powered MNMs, most of the light-driven MNMs are fuel-free motors, which are composed of one or more photoactive materials including photothermal materials, photocatalytic materials, photochromic materials, *etc.*[70] Therefore, light-driven MNMs can be divided into light-induced self-thermophoretic MNMs,[71] light-induced chemically reactive MNMs,[72] and light-induced isomerized MNMs[73] according to the reaction mechanism (Fig. 1).

2.1 Light-induced self-thermophoretic MNMs

Light-induced self-thermophoretic MNMs with photothermal materials can absorb light energy and convert it into thermal energy, thereby generating a temperature gradient to trigger MNMs' propulsion. The motors are mainly based on photothermal materials such as carbon nanomaterials, precious metals Au, platinum (Pt), *etc.* which are commonly used alone or in combination with other photocatalytic materials.[80] Photothermal materials can produce photothermal effects under light irradiation, so they can be used to develop light-driven MNMs.[81] The photothermal effect is the conversion of light energy into heat energy. When light acts on the surface of a substance, electrons in the substance absorb the energy of the photons and are excited. These excited electrons transfer their energy to the molecules of the substance through collisions and other processes, which accelerate their vibration and rotation, thus generating heat energy.[82] This type of motor is generally designed as a Janus structure with a partially absorbing coating[25,83] or two photothermal materials with different absorbing properties.[75,84] Under continuous light irradiation, such materials generate asymmetric absorption which creates a temperature gradient on the surface of the MNMs, leading to self-induced thermophoretic motion.[85]

For example, Zheng *et al.* reported a near-infrared (NIR) light-driven Janus mesoporous silica nanomotor (JMSN).[86] The JMS nanomotors were constructed by depositing Au on the hemispherical surface of gadolinium-doped mesoporous silica nanoparticles. As a widely used metal material, Au had good photothermal conversion ability. Due to the asymmetric thermal gradient generated by the Au half-shell, the JMS nanomotors were able to exhibit autonomous thermal propulsion under NIR irradiation. The diffusion coefficient of JMSN without NIR light is ≈0.14 μm s^{-2}, while the diffusion coefficient under 2.5 W cm^{-2} NIR irradiation reached ≈3.49 μm s^{-2}. The substantially enhanced diffusion of JMS nanomotors under low-intensity NIR irradiation realized efficient tumor penetration and promoted magnetic resonance imaging *in vivo*. In the biomedical field, light-driven MNMs are usually combined with photodynamic therapy (PDT). Cao *et al.* presented hybrid phototactic/phototherapeutic nanomotors triggering autonomous propulsion and simultaneous phototherapeutic generation of reactive oxygen species (ROS) (Fig. 2A).[87]

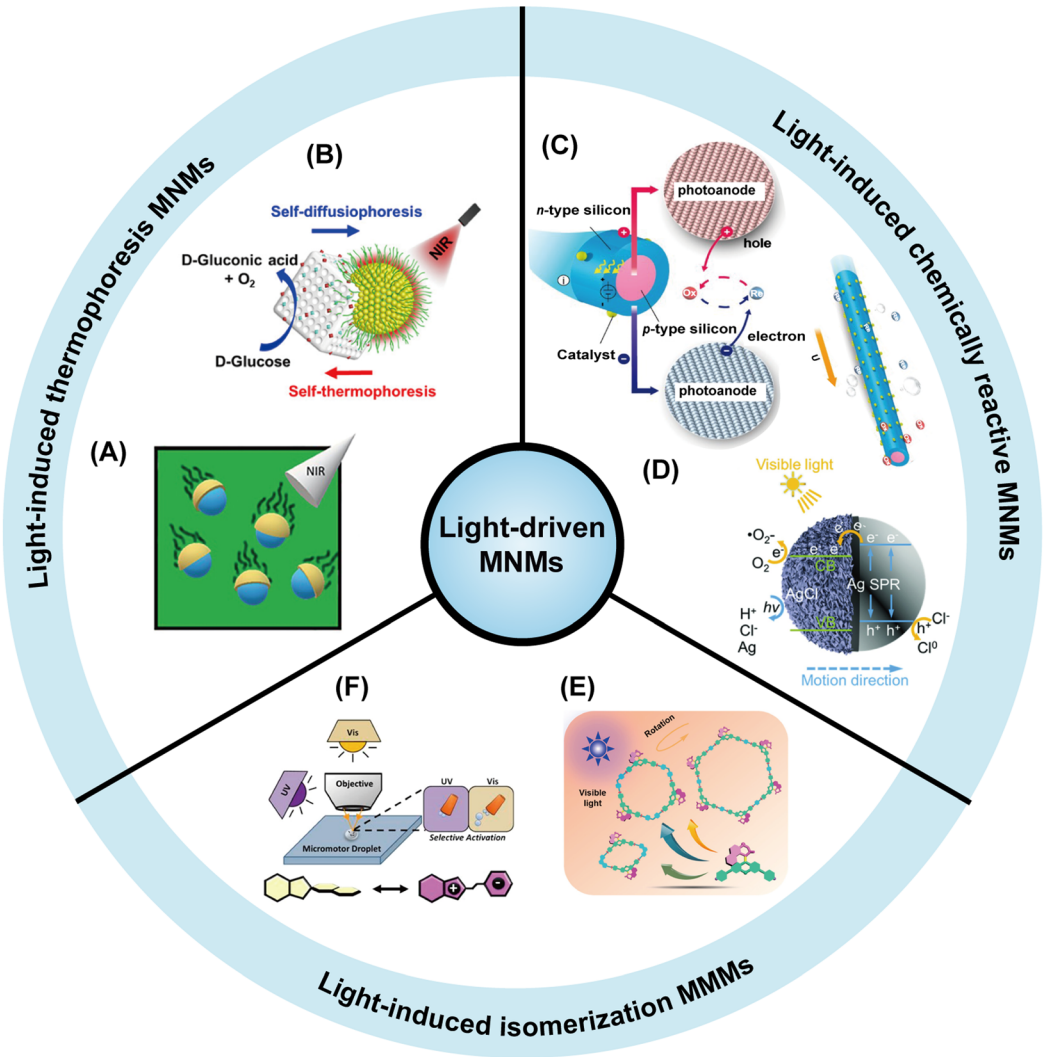

Fig. 1 Light-driven MNMs with three different propulsion mechanisms. The pictures are presented clockwise from left to right. Light-induced thermophoretic MNMs: (A) the SiO_2–Au nanomotors exhibit efficient self-propulsion when exposed to near-infrared (NIR) irradiation. Reproduced with permission.[74] Copyright 2023, Wiley-VCH GmbH. (B) A SiO_2@Au core@shell nanosphere driven by thermal electrophoresis under NIR light irradiation. Reproduced with permission.[75] Copyright 2022, American Chemical Society. (C) A light-driven microswimmer that converts incident photons into mechanical propulsion with the aid of redox shuttles. Reproduced with permission.[76] Copyright 2020, American Chemical Society. (D) An ultraviolet (UV) light-driven Ag/AgCl-based spherical Janus micromotor, which couples plasmonic light absorption with the photochemical decomposition of AgCl. Reproduced with permission.[77] Copyright 2018, Wiley-VCH. (E) A VIS-light-triggered bipyridine molecular motor ligand MPY. Reproduced with permission.[78] Copyright 2021, American Chemical Society. (F) A spirochetal nanomotor that controls molecular switching by UV and VIS light irradiation. Reproduced with permission.[79] Copyright 2016, American Chemical Society.

The hybrid nanomotors were based on aggregation-induced emission (AIE) polymersomes coated with an asymmetric plasmonic Au shell. Due to the asymmetric structure, AIE/Au polymersomes achieved self-thermophoresis propulsion through two-photon near-infrared (TP-NIR) activated plasmonic heating. Compared with control Au-coated polymersomes, which did not contain structural AIE moieties, the velocities of the AIE/Au nanomotors were up to 45% and proportional to the intensity of light. Combining the properties of both AIE and Au, the hybrid nanomotors realized increased efficacy and enhanced cytotoxic response upon targeted NIR irradiation. Unlike metal nanoparticles, the photophysical properties of organic semiconducting polymer nanoparticles (SCP NPs) are less size-dependent.[88] Therefore, they are often used in cancer therapy and bioluminescent imaging as multifunctional photothermal agents.[89] Huang *et al.* reported a kind of photoactivated organic nanomachine with asymmetric geometry (Fig. 2B).[90] The nanomachines were assembled using a completely organic SCP as an engine which played a role in light-to-heat conversion and methacrylate-based copolymers as a macromolecular prodrug payload. The organic nanomotors were activated to produce an asymmetric thermal gradient for self-propulsion under NIR irradiation. Without irradiation, the NPs showed a typical Brownian

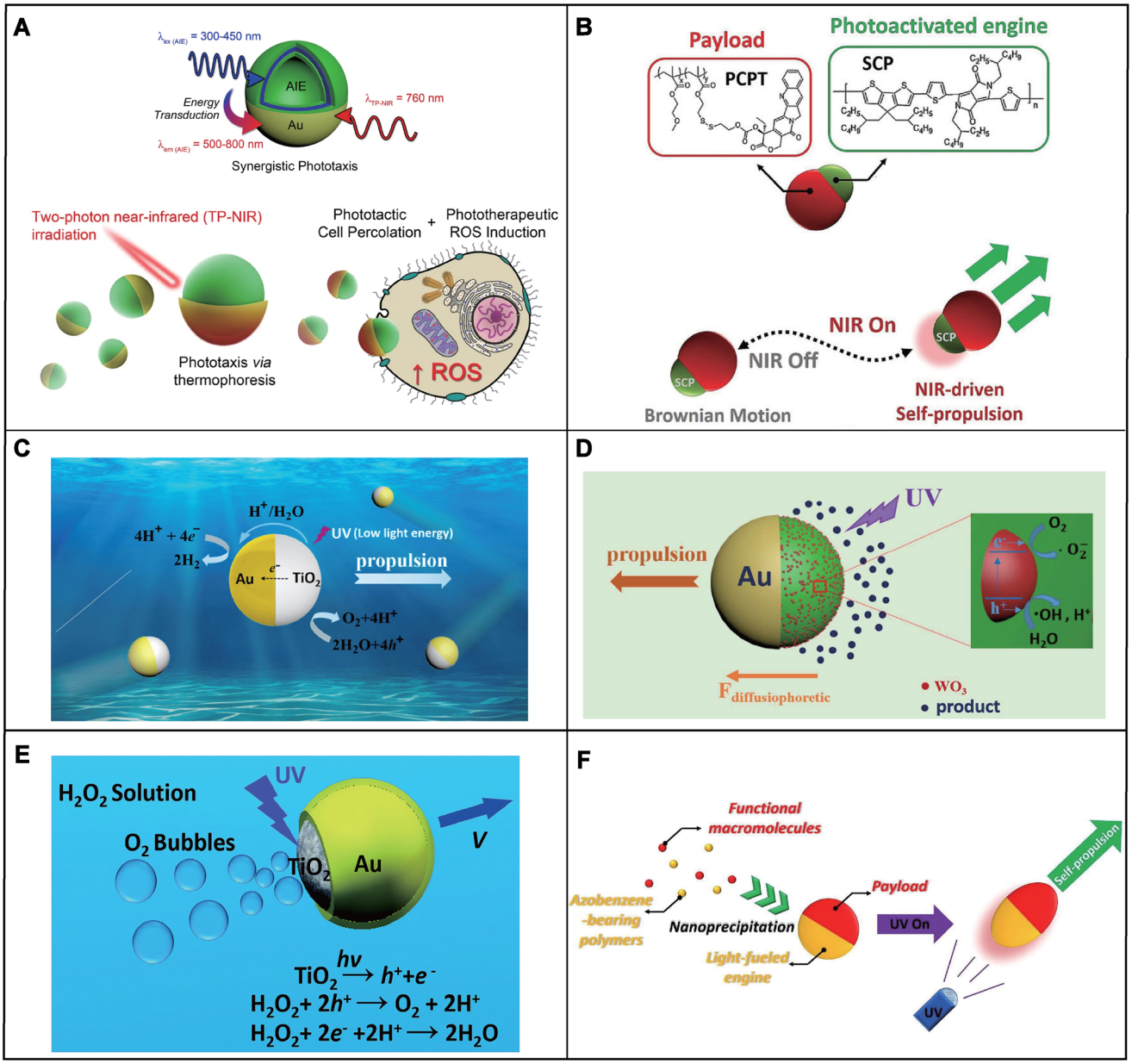

Fig. 2 Classification and mechanism of light-driven MNMs. (A) Dual behavior and synergistic motion of nanomotors triggered by direct and indirect activation of the plasmonic Au shell. Reproduced with permission.[87] Copyright 2021, Springer Nature. (B) Process of organic semiconducting nanomotors in response to NIR on/off. Reproduced with permission.[90] Copyright 2022, Wiley-VCH GmbH. (C) Mechanism of catalytic TiO_2–Au Janus micromotors powered by UV light in water. Reproduced with permission.[97] Copyright 2015, American Chemical Society. (D) Schematic of the driving mechanism of light-driven Au-WO_3@C sphere Janus micromotors. Reproduced with permission.[99] Copyright 2017, American Chemical Society. (E) The schematic demonstration of the UV-driven motion of the Am-TiO_2/Au Janus micromotor in the H_2O_2 solution. Reproduced with permission.[93] Copyright 2016, The Royal Society of Chemistry. (F) Azobenzene-bearing polymer engine powered organic nanomotors. Reproduced with permission.[107] Copyright 2022, Elsevier.

movement with an average velocity of 2.1 μm s^{-1}, while NPs obviously accelerated to 6.1 μm s^{-1} after 6 s of NIR irradiation (808 nm, 1 W cm^{-2}). The excellent motion performance of the semiconducting polymer engine-powered nanomachines makes it possible to carry therapeutic cargoes through the physiological barrier and significantly improve tumor penetration.

Light-induced self-thermophoretic MNMs have been widely studied due to their ease of preparation and simplicity of operation. The fact that they do not need fuel and do not produce waste gives them significant advantages in biomedical applications. In order to promote effective MNMs' movement, it is necessary to apply high-intensity light which may lead to potential heat damage to living tissues. However, for self-ther-

mophoretic MNMs, the potential damage to biological tissue caused by heat generated to promote efficient motor movement needs to be considered.

2.2 Light-induced chemically reactive MNMs

NIR is often used to induce self-thermophoretic MNMs to promote movement,[91,92] while the motion of light-induced chemically reactive MNMs is generally triggered by ultraviolet (UV)[93,94] and visible (VIS) light.[63,77] The MNMs are based on photocatalytic and photosensitive materials that produce chemical reactions under light causing an electrolyte or non-electrolyte gradient to drive motion.[95] The motion mechanism of these motors can be divided into self-electrophoresis, electrolyte diffusiophoresis and non-electrolyte diffusiophoresis.

Among light-driven MNMs, photocatalyst-based MNMs are the most extensively studied due to the advantages of strong propulsion and photochemical stability. Photocatalytic materials mainly include metal–oxide semiconductors, such as titanium dioxide (TiO_2), which can catalyse reactions under irradiation resulting in the asymmetric generation or depletion of ions on the motor surface.[96] Due to the asymmetric distribution of ions, an ion gradient is generated to form a local self-generated electric field (E), and thus the charged MNMs move in response to the self-generated E.[70] This motion behavior is described as self-electrophoresis. For instance, Dong *et al.* reported UV light-driven TiO_2–Au Janus micromotors which consisted of ordinary TiO_2 microparticles coated with asymmetrical Au metal (Fig. 2C).[97] Under UV irradiation, a redox reaction happened on the TiO_2 hemispheres of the micromotors, consuming water to produce protons. The resulting H^+ flowed towards the Au hemisphere, which generated a slip velocity to push the micromotors forward. The TiO_2–Au Janus micromotors based on self-electrophoresis achieved efficient propulsion (over 25 body length per s) under an extremely low UV light intensity (40 mW cm^{-2}). The attractive fast movement triggering response and low light energy requirement of the TiO_2–Au Janus photocatalytic micromotor hold considerable promise in biomedical applications.

Besides, photosensitive materials include some inorganic salts, such as silver halides (AgX, X = Br, Cl, or I), which can produce cations and anions with different diffusivities in aqueous solutions under ultraviolet light creating an electrolyte concentration gradient around the motors.[80] The solute concentration gradient in the fluid creates a diffusion-induced electric field, resulting in electrolyte self-diffusion electrophoresis that powers MNMs' motion.[98] For example, Ren *et al.* designed a novel light-driven Au-WO_3@C Janus micromotor based on colloidal carbon WO_3 nanoparticle composite spheres with an asymmetrical Au coating (Fig. 2D).[99] When exposed to UV light, the photocatalyst could react with oxygen and water to initiate complex radical chain reactions and produce various products such as H_2O_2, H^+, $^{\bullet}OH$, and O_2^-. The discontinuous structure formed by the WO_3 nanoparticles absorbed on the surface of microspheres limited the electron transfer from the semiconductor to the metal, leading to a higher concentration of products around the WO_3 side in comparison with the Au side. This created an osmotic flow from low to high solute concentration regions; therefore, the micromotors were propelled pointing to the Au side through the electrolyte diffusiophoresis mechanism.

In addition to creating electrolyte gradients through photoinduction, certain photocatalysts can produce neutral molecules by asymmetric photocatalytic reactions to construct non-electrolyte gradients, which can also be used to design light-driven MNMs.[70] This type of motor is based on non-electrolyte diffusiophoresis to propel motion. Similar to other light-driven MNMs, these motors are usually also designed with an asymmetric Janus structure. For instance, Guan *et al.* proposed a bubble-propelled photoactivated amorphous TiO_2/Au (Am-TiO_2/Au) Janus micromotor with an asymmetrically coated Au layer on the exposed surface (Fig. 2E).[93] Under UV irradiation, oxygen molecules produced by the efficient photocatalytic H_2O_2 decomposition over the micromotors undergo diffusiophoresis in the H_2O_2 solution. The generated oxygen molecules interacted with the surface of the micromotors, creating an asymmetric non-electrolyte gradient that powers the motion of the micromotors.

Light-induced chemically reactive MNMs have the advantages of fast motion speed, stable movement, and controllable direction, and the photocatalyst TiO_2 has been extensively used in light-driven MNMs due to its chemical stability, low-cost, and nontoxic nature. However, due to the poor penetration performance of UV-VIS light, the application of this kind of motor *in vivo* is limited.

2.3 Light-induced isomerized MNMs

Light-induced isomerized MNMs are mainly composed of special photochromic materials which can respond to light stimulation by changing their molecular structure.[95] Their structure can be restored to its original state after the light source is removed or the wavelength of the light is changed.[100] The transformation mechanisms are generally based on different kinds of reversible reactions, such as *cis–trans* isomerization, electron transfers (oxidation–reduction), intramolecular hydrogen transfers and photoionization.[101] Commonly, azobenzenes and spiropyrans have been used in MNMs owing to their good chemical stability.[102,103] For azobenzenes, the exposed surface of the *cis* isomer has a higher surface free energy than the *trans* isomer.[70] Therefore, under the irradiation of UV and VIS light, the *trans–cis* isomerization of azobenzene generates a surface energy gradient to drive the motion of MNMs.[104,105] For spiropyrans, the photoinduced pericyclic reaction changes the polarity of the structure, which alters the interfacial tension with the medium, inducing an interfacial tension gradient.[101,103] As a consequence, the interfacial tension gradient acts as a driving force to propel MNMs. However, this structure is generally not used to drive the nanomotor movement alone but is usually used to play an auxiliary role to modulate the motion performance of hybrids with other driving mechanisms playing the main role.[79,106]

For example, Xiong *et al*. reported a polymeric nanomotor with an azobenzene polymer as the engine (Fig. 2F).[107] Upon

Table 1 Applications of light-driven MNMs

Micro/nanomotor type	Propulsion mechanism	Application	Ref.
MSN/Pt@PEG-Glu@SAM, 81.1 ± 4.9 nm in diameter	Self-thermophoresis	Autonomous mucus penetration and oral targeted therapy of colorectal cancer	109
CuS/TiO_2@PEGTf@BMS, 178.9 ± 6.0 nm in diameter	Self-thermophoresis	Enhance intestinal mucus penetration and reduce pathogenic bacteria interception in colorectal cancer	60
Janus-type polyelectrolyte microcapsules coated with an erythrocyte membrane	Self-thermophoresis	Thrombus ablation	110
PCL and PLGA coated VIS-driven micromotors	Self-diffusiophoresis	Effectively adsorb and remove two septicaemia related toxins from the blood	62
JN@MnO_2@hQN, 93.4 nm in diameter	Self-thermophoresis	*In situ* imaging of miRNAs in living cells	111
MSN-based Janus nanomotors with a gold half-shell	Self-thermophoresis	Improve the blood–brain barrier penetration and regulate protein aggregation in the body	61
Parachute-like nanomotors based on Pt NPs, 80 nm in diameter	Self-thermophoresis	Enhance skin penetration and antifungal therapy	112
Double plasma (AuNR-SiO_2-Cu_7S_4) nanomotors	Self-thermophoresis	Enhance the transdermal penetration and treat deep-seated drug-resistant bacterial infections	63
mPL-Pc@PDA Janus nanomotors, 214 nm in diameter	Self-thermophoresis	Promote deep penetration in the tumors and produce long-lasting synergistic PDT and PTT for tumor treatment	113
NIR light-driven JMS nanomotors	Self-thermophoresis	Precise cancer diagnosis and MR imaging	86
Mesoporous–macroporous silica/platinum nanomotors	Self-thermophoresis	Deep penetration of tumors and combined photothermal or chemotherapy treatments	114
N-doped jellyfish-like mesoporous carbon nanomotors coordinated with single-atom copper	Self-thermophoresis	Improve solid tumor penetration and tumor inhibition	25
Organic nanorockets containing a semiconducting polymer and thermo-driven macromolecules, 105 nm in diameter	Self-thermophoresis and self-diffusiophoresis	Traverse various physiological obstacles in the tumor microenvironment and enhance the antitumor efficacy	115
Mesoporous SiO_2/Au nanomotors, 306 nm in diameter	Self-thermophoresis	Eradication of *Pseudomonas aeruginosa* (*P. aeruginosa*) biofilms	74
ZnO : Ag PVD-free micromotors	Self-electrophoresis	Eradication of *P. aeruginosa* and MRSA bacterial biofilms	116
B-TiO_2/Ag nanorobots, 400 nm in diameter	Self-electrophoresis	Remove bacterial biofilms grown onto titanium miniplate implants	117
MMS/Au/PTX/VEGF nanotubes	Self-thermophoresis	Promote penetration into the plaque site and alleviate the development of atherosclerosis	66
CD-LA-Au-aV dual-drive nanomotors, 191 nm in diameter	Self-thermophoresis and bubble propulsion (NO)	Penetration into the plaque and anti-atherosclerotic therapy	118
Janus aminated mesoporous silica nanomotors with a Pt asymmetric coating, 450 nm in diameter	Self-thermophoresis	Promote deep penetration into the plaque and treat atherosclerosis	119

UV irradiation, the motor absorbed the light to trigger the photothermal conversion and photoisomerization, the former creating a thermal gradient to induce self-thermophoresis and the latter leading to internal mass migration resulting in significant particle deformation that was able to elongate the thermal gradient surrounding the nanoparticles. Thermophoresis played a dominant role in the locomotion, and photoisomerization had an extra promotion effect on the propulsion which made a synergetic contribution to the light-driven nanomotors. Although light-induced isomerized MNMs do not use isomerization as the main driving force, it is still an important part of light-driven MNMs due to its function to turn on or off as well as modulate the motion.

Light as an attractive external energy source has been used as a direct stimulus or an auxiliary energy source to control motor motion through different propulsion mechanisms. The light-induced thermophoretic MNMs can generate thermal gradients through asymmetric photothermal conversion within motors for thermophoresis. Differently, light-induced chemically reactive MNMs create a chemical (electrolyte or non-electrolyte) concentration gradient around the MNMs by asymmetric chemical reactions with the surrounding medium to power self-electrophoresis. The light-induced isomerized MNMs can switch the structure of motors with *trans–cis* transformation to realize the "on" or "off" of motors and play a synergistic propulsion role with other motors. Light-driven MNMs have several advantages: (1) remote control of motor movement in a non-invasive manner, (2) control of the speed of the motors by the light intensity, and (3) fast on/off control of motor motion. Therefore, light-driven MNMs are widely studied and applied in environmental remediation, sensing, and biomedicine. Next, the applications of light-driven MNMs in the biomedical field are introduced in detail.

3. Applications of light-driven MNMs

In recent years, light-driven MNMs have been studied as promising intelligent transporters for drug delivery, *in vivo* imaging, and photothermal therapy in the biomedical field. Although the functions of MNMs are gradually diversified, physiological barrier penetration is still their biggest application field.

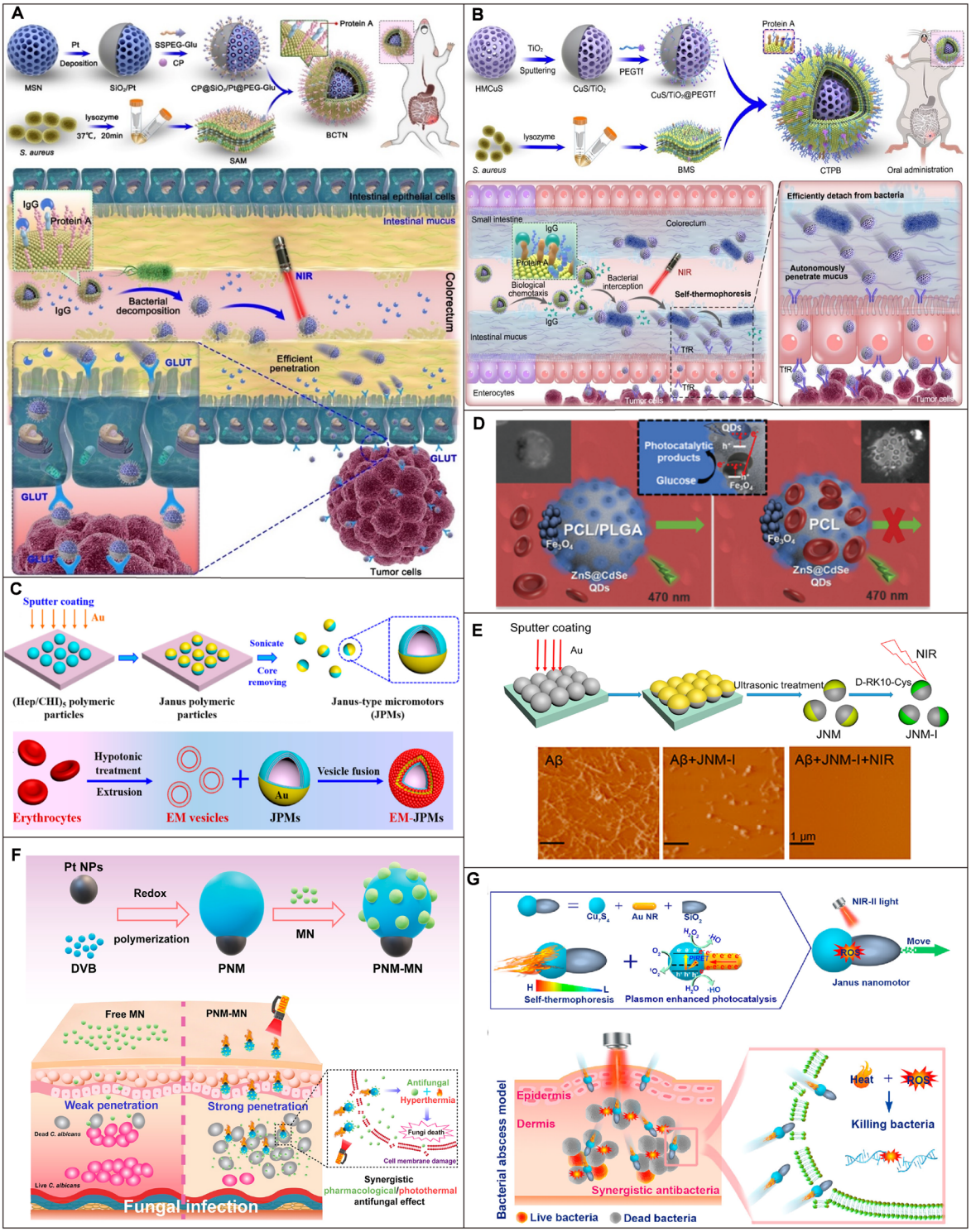

Fig. 3 Application of MNMs in penetrating intrinsic barriers *in vivo*. (A) Schematic illustration of the synthetic procedure and CRC therapy of BCTN. Reproduced with permission.[109] Copyright 2022, The American Association for the Advancement of Science. (B) Schematic illustration of self-thermophoretic nanoparticles enhancing intestinal mucus penetration and reducing pathogenic bacteria interception in CRC. Reproduced with permission.[60] Copyright 2023, Wiley-VCH GmbH. (C) Schematic diagram of the synthesis and thrombolytic action of EM-JPMs. Reproduced with permission.[110] Copyright 2018, American Chemical Society. (D) Schematic illustration of the navigation of light-driven CdSe@ZnS QD Fe_3O_4 NP Janus micromotors in diluted blood with a PCL/PLGA (left) and (right) PCL polymer body. Reproduced with permission.[62] Copyright 2021, The Royal Society of Chemistry. (E) Schematic diagram of the preparation and inhibition of Aβ aggregation of JNM-I. Reproduced with permission.[61] Copyright 2020, American Chemical Society. (F) Schematic illustration of the preparation of a NIR laser-driven parachute-like nanomotor PNM-MN and its synergistic antifungal effects. Reproduced with permission.[112] Copyright 2021, American Chemical Society. (G) Schematic illustration of Janus structure preparation for AuNR-SiO_2-Cu_7S_4 nanomotors and its effective treatment of MRSA infection. Reproduced with permission.[63] Copyright 2023, American Chemical Society.

Compared with traditional nanodrugs, light-driven MNMs can cross various biological barriers to achieve effective drug delivery due to their non-invasive and controllable motion properties.[108] Among them, NIR light-driven MNMs play a dominant role because of the high transmittance of NIR light in biological tissues. In this section, recent advances in the use of MNMs to bypass biological barriers for the treatment of various diseases are presented (Table 1).

3.1 Intrinsic barrier *in vivo*

There are several physiological barriers that protect organisms from foreign substances such as the gastrointestinal mucus barrier and the blood–brain barrier. Meanwhile, the barriers also prevent the drug from reaching the pathological site to produce sufficient pharmacological activity. Therefore, designing motors that can pass through physiological barriers without imposing an additional burden on the living body is extremely challenging.

3.1.1 Mucus barrier. Intestinal mucus is an important biological barrier that protects intestinal epithelial cells from being exposed to the complex intestinal environment and microbial invasion and helps maintain homeostasis in the intestine.[120] Mucus is composed of water (~95%), glycoproteins (mucins, ~2–5% w/v), lipids, DNA, antibodies, and cellular debris, and is essentially a viscoelastic gel layer.[121] Mucins are flexible, high molecular weight protein polymers secreted by goblet cells that cross-link with each other to form a mucus skeleton.[122,123] Mucus spreads throughout the gut, selectively filtering foreign substances to limit pathogen access to epithelial cells.[124] The thickness of human small intestinal and colon mucus is about 15 μm (ref. 124) and 110–160 μm,[122] respectively. Besides, the rate of intestinal mucus clearance is high, which sets a limited time frame for efficient drug delivery.[125] Hence, intestinal mucus is one of the major barriers to the absorption of oral nanomedicines due to its shielding and lubrication functions.

Light-driven MNMs have been developed for deep penetration of intestinal mucus to improve drug bioavailability. Wang *et al.* proposed a biological chemotaxis-guided self-thermophoretic nanoplatform (BCTN) for autonomous mucus penetration in the targeted therapy of colorectal cancer (CRC) (Fig. 3A).[109] The nanoplatform introduced mesoporous silica nanoparticles (MSNs) as a matrix sprayed with Pt on the hemispheres to construct asymmetric structures (SiO_2/Pt) and then was covered with a *Staphylococcus aureus* biomimetic membrane (SAM), which could specifically target the intestinal inflammatory environment of colorectal cancer (CRC). The nanomotor asymmetrically absorbed the NIR laser to produce the self-thermophoretic effect which drove it to penetrate the colon mucus barrier autonomously. Compared with ordinary SiO_2/Pt nanoparticles, the bioavailability of the light-driven nanomotor increased by 2.6 fold, which provided new insight into the non-destructive penetration of complex biological barriers and effective oral targeted therapy of CRC.

Similarly, the team presented a light-induced self-thermophoretic nanomotor (CTPB) with faster speed which enhanced intestinal mucus penetration and reduced pathogenic bacteria interception in CRC (Fig. 3B).[60] The nanoplatform was based on hollow mesoporous copper sulfide sprayed with titanium dioxide asymmetrically (CuS/TiO_2), and the biomimetic membrane of *Staphylococcus aureus* (BMS) was employed to camouflage the nanoparticles. Under NIR laser irradiation, the self-thermophoresis of nanoparticles after asymmetric absorption of the NIR laser to form a thermal gradient drove the motor to rapidly penetrate the intestinal mucus and improve the drug delivery efficiency. The intestinal mucus penetration efficiency was increased by 2.7 fold and the pathogenic bacteria interception was decreased by 3.5 fold with the movement of the motor. Both the light-driven nanomotors augmented CRC therapy through efficient intestinal mucus penetration by self-thermophoretic propulsion, which provided a simple and universal strategy for targeted oral drug delivery.

3.1.2 Hemorheological barrier. MNMs, which are able to swim in the blood, can penetrate deep into the body through the vascular system. The maximum velocity of MNMs is usually several orders of magnitude slower than the velocity of blood flow,[126] so it is difficult to achieve the controlled movement of MNMs in the blood countercurrent. Therefore, it is a challenge for them to move autonomously in the circulatory system. To operate in the blood circulation system, MNMs should meet at least two requirements. First, the propulsion has to be strong enough to drive them through the viscous, multi-component blood.[127] Second, the smallest capillaries are only a few micrometers in diameter.[128] This requires the size of the synthetic MNMs to be smaller than the diameter of the blood vessels that they pass through and suitable for breaching biological barriers in the blood circulatory system; otherwise there is a risk of blocking the brain or pulmonary artery.[39]

As the most abundant cell in the blood, red blood cells with their physical and chemical properties are essentially biocompatible, degradable, and non-immunogenic materials and exhibit long circulating behavior in the physiological environment.[111,129] Therefore, to further reduce undesirable interactions with the immune system, MNMs can be decorated with a cell-derived coating. Shao *et al.* reported erythrocyte membrane-coated Janus polymeric motors (EM-JPMs) driven by NIR laser irradiation, which were successfully applied in thrombus ablation (Fig. 3C).[110] The template silica particles were exposed to chitosan (CHI) and heparin (Hep) solutions, which were self-assembled layer by layer, and Au was unsymmetrically sputtered on the surface of MNMs to prepare asymmetric structures (JPMs) and then covered with erythrocyte membranes to introduce the physical and chemical characteristics and biological functions of red blood cells. The movement speed of EM-JPMs in serum and blood under NIR irradiation was 3.52 μm s^{-1} and 2.33 μm s^{-1}, respectively, which was faster than that of bare JPMs. In addition, they had a good therapeutic effect on thrombus ablation.

Pacheco *et al.* reported VIS-driven micromotors (PCL/PLGA) coated with polycaprolactone (PCL) and polylactic-*co*-glycolic acid (PLGA), encapsulated CdSe@ZnS quantum dots as photoresponsive materials and asymmetric Fe_3O_4 nanoparticle patches to achieve efficient propulsion (Fig. 3D).[62] Under VIS irradiation, an electron moved towards the quantum dot regions and recombined with the electronic levels of the Fe_3O_4

NPs to form holes, which decomposed glucose and led to the accumulation of photodegradation products, thus driving the movement of the micromotor. Because the PLGA layer prevented red blood cell adhesion and protein adsorption, the speed of the PCL/PLGA micromotors in the blood was about 8.2 ± 2.4 μm s^{-1}, while the speed of the PCL micromotors dropped to 2.6 ± 0.2 μm s^{-1}, about 1/3 of the speed of the PCL/PLGA micromotors. In addition, PLGA-coated micromotors in blood samples had 70–90% removal rates for *Escherichia coli* toxin and α-bungarotoxin, while PCL micromotors had negligible removal rates. This was also a step forward for light-driven MNMs in biomedicine.

3.1.3 Blood–brain barrier. The blood–brain barrier (BBB) is one of the physiological barriers that limit drug delivery.[130] It is present in all well-developed microorganisms of the central nervous system, and it is mainly composed of microvascular endothelial cells, astrocytes, and pericytes.[131] Basically, 100% of macromolecular drugs and >98% of small-molecule drugs find it difficult to cross the BBB.[132] In order to safely and efficiently deliver drugs into the brain, various strategies have been developed to overcome the BBB, including BBB disruption, receptor-mediated transcytosis, carrier-mediated transcytosis, cell-mediated transport, *etc.*[30,133] Although extensive achievements have been made in this field, it still faces challenges such as low drug loading and poor targeting.[134] Research has shown that nanomotors can improve the efficiency of drug delivery. For example, Wan *et al.* constructed a nitric oxide (NO)-driven nanomotor (Ang-PAMSe), which could effectively penetrate the BBB for glioblastoma treatment.[135] Therefore, MNMs that can actively move and target drug delivery are hopeful to provide a new solution for crossing the BBB.

Recently, Liu *et al.* developed a NIR-propelled Janus nanomotor (JNM) to enhance the inhibition/modulation of Aβ aggregation (Fig. 3E).[61] The MSNs were selected as the carrier of the nanoplatform and Au was unsymmetrically sputtered on the surface of the MSNs to prepare an asymmetric structure, and then the Aβ-targeting peptide inhibitor D-RK10-Cys was conjugated to the Au part of the JNM *via* Au–S bonds to form JNM-I. The average speeds for JNM-I reached 5.3 μm s^{-1} and 6.7 μm s^{-1} respectively under the irradiation of 0.98 W cm^{-2} and 1.96 W cm^{-2} NIR. In addition, stronger BBB penetration of JNM-I was significantly observed after NIR irradiation compared to the group without NIR irradiation. This nanomachine opened new possibilities for regulating protein aggregation and drug delivery in the body.

3.1.4 Skin barrier. The skin provides physical, chemical, microbiological, and immune barriers against a variety of injuries, such as infections.[136] Fungal infections, a growing clinical problem worldwide, cause about 1.5 million deaths each year.[137] The surface of the skin is the most common site of fungal infection. Topical antifungal treatments are often effective at treating superficial fungal infections. However, after the fungi infect the skin, they subsequently migrate to deeper tissues through the stratum corneum (SC) and cause inflammation.[138] Due to the barrier function of the skin, the speed and depth of passage of drugs, used to treat local infections, through the skin is significantly affected, which is a major obstacle to antifungal treatment.[139] In order to address these problems, MNMs have attracted great attention as an effective antifungal treatment strategy.

For example, Ji *et al.* reported a NIR laser-propelled parachute-like nanomotor (PNM) loaded with miconazole nitrate (MN) to form PNM-MN, thereby enhancing transdermal drug delivery and achieving antifungal synergistic therapy (Fig. 3F).[112] The PNM was synthesized by a one-step method using Pt nanoparticles (Pt NPs) as a photothermal agent and PDVB as a thermal insulation rubber. MN was loaded on the PNM parachute canopy through hydrophobic interaction. In Dulbecco's modified Eagle's medium (DMEM), the velocity of the PNM irradiated by an NIR laser could reach 24.69 ± 1.88 μm^2 s^{-1}, which was about 4.5 times faster than the PNM without NIR laser irradiation. *In vivo* experiments showed that the penetration efficiency of the PNM irradiated by NIR reached 69.96% in the dermis, while the PNM without NIR irradiation was only 18.41%, which could effectively kill *Candida albus* and accelerate the elimination of abscesses. Therefore, NIR laser-propelled PNM-MN, as an antifungal nanomedicine, provided a promising strategy for transdermal drug delivery and antifungal therapy.

For human tissues, less than 10 mm penetration could be realized by VIS and NIR light, which hinders phototherapy to deep lesions.[140] In recent years, the second NIR window (NIR-II, 1000–1700 nm) was developed for deep imaging and therapy up to ~14 mm compared to ~7 mm of traditional NIR (650–900 nm).[141] Currently, Liu *et al.* developed a NIR-II light-driven double plasma (AuNR-SiO_2-Cu_7S_4) antibacterial nanomotor by overgrowing Cu_7S_4 nanocrystals at a high curvature site of Au nanorods (Fig. 3G).[63] Because of the plasma coupling effect and enhanced energy transfer, an enhanced local photothermal field was formed close to the AuNR-Cu_7S_4 interface under the irradiation of NIR-II. Therefore, the nanomotors could be actively driven by self-thermophoresis. The nanomotors showed a motion speed of about 9.8 μm s^{-1} driven by low-power NIR-II light (0.75 W cm^{-2}). The cross-sectional PAI images of mouse skin showed that the nanomotors could penetrate the skin epidermis and enter the dermal region to a depth of about 1.5 mm under NIR-II light irradiation. More importantly, it showed excellent bactericidal activity against *Staphylococcus aureus* (MRSA), providing ideas for the treatment of deep bacterial infections.

3.2 Disease-associated barriers

In addition to the inherent barriers in the human body, the associated biological barriers will also be formed along with the production of diseases, such as the dense extracellular matrix (ECM) outside tumors,[142,143] atherosclerotic plaques,[8] and bacterial biofilms in bacterial infections,[144] which can affect the efficiency of drug delivery and in turn reduce the effectiveness of the drugs. In recent years, MNMs with excellent motion properties have been used to penetrate and even remove these barriers that accompany disease. The application of MNMs to some disease-associated barriers will be introduced in detail in the following sections.

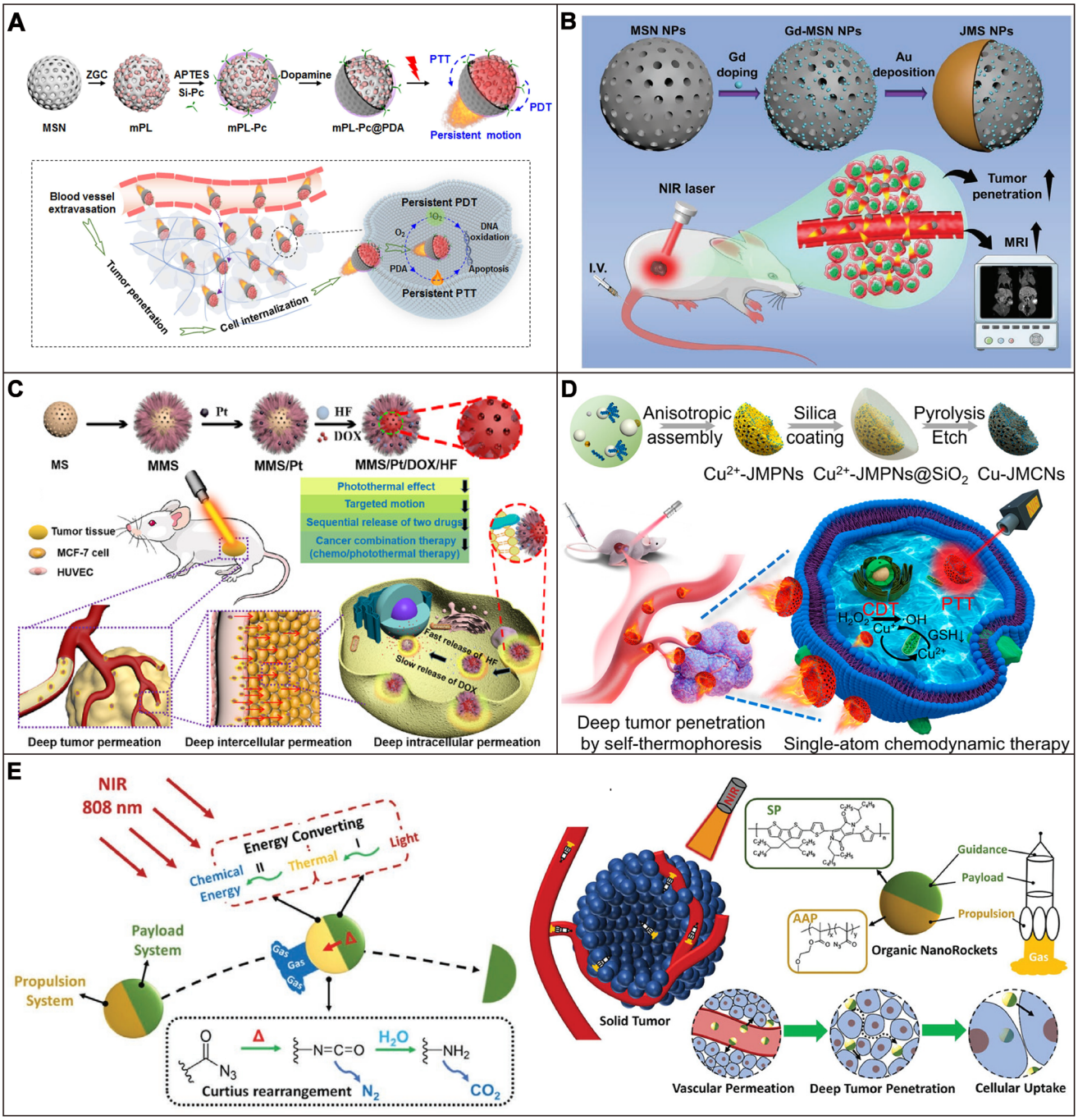

Fig. 4 Application of MNMs in penetrating tumor tissue barriers. (A) Schematic illustration of the preparation of mPL-Pc@PDA nanomotors and their application in improving vascular exosmosis, tumor penetration, and cell internalization. Reproduced with permission.[113] Copyright 2022, Elsevier B.V. (B) Schematic illustration of the preparation process of JMS nanomotors and the NIR powered JMS nanomotors for tumor deep penetration and enhanced MR imaging. Reproduced with permission.[86] Copyright 2021, Wiley-VCH GmbH. (C) Schematic illustration of the preparation of multifunctional MMS/Pt/DOX/HF nanomotors and their application in cancer therapy. Reproduced with permission.[114] Copyright 2020, Wiley-VCH GmbH. (D) Schematic illustration of the synthesis process of Cu-JMCNs and their enhancement of tumor penetration and therapy under NIR light irradiation. Reproduced with permission.[25] Copyright 2023, American Chemical Society. (E) Schematic illustration of organic nanorockets and their application in deep tumor penetration. Reproduced with permission.[115] Copyright 2023, Wiley-VCH GmbH.

3.2.1 Tumor tissue barrier. The complex tumor microenvironment shows an uneven distribution of high interstitial pressure, cell membrane barriers, and dense tumor tissues.[143,145] These barriers prevent nanomaterials from penetrating deeper into tumor tissues and lead to uneven distribution and reduced enrichment of nanomaterials in tumors.[146] Studies have shown that the amount of nanoparticles delivered to the tumor site is very limited.[12]

Therefore, it is very important to improve the infiltration efficiency of nanoparticles in tumors. MNMs can load anticancer drugs through biological barriers and reach targeted cells through autonomous navigation, which can greatly improve the efficiency of anticancer drug delivery.

At present, phototherapy techniques, such as PDT and photothermal therapy (PTT), have aroused great interest.[147] But they face the challenges of low accumulation and penetration of photosensitizers in tumors and dose-dependent side effects.[148] To address this problem, persistent luminescence (PL)-activated nanomotors with the integration of PL-illuminated PTT and PDT were developed by Zhang *et al.* (Fig. 4A).[113] First of all, ZnGaO : Cr (ZGC) PL nanodots were deposited on mesoporous silica nanoparticles, coupled with silicon phthalocyanine as a photosensitizer (mPL-Pc) and coated with polydopamine (PDA) to prepare Janus mPL-Pc@PDA NPs. PL activated PDA layers to produce a thermal gradient around the Janus NPs, which drove the nanomotor movement. The photothermal effect of Janus mPL@PDA NPs resulted in a motion velocity of 6.10 μm s^{-1}, which was significantly greater than that of mPL-PC@PDA (1.5 times) and mPL (3.1 times) NPs. The PDT of Janus NPs under PL irradiation continued to produce intracellular ROS to damage tumor cells, and the accumulation and penetration of Janus NPs in the tumor increased significantly.

Up to now, most nanomotors have a single porous structure. For example, Zheng *et al.* prepared a JMSN by depositing Au on a hemispherical surface of gadolinium-doped MSN NPs; its penetration into cells and tumor tissues was significantly enhanced under low intensity NIR irradiation (Fig. 4B).[86] In order to enhance the ability of MNMs to carry drugs with different functions, Wan *et al.* proposed a novel type of mesoporous–macroporous silica/platinum nanomotor (MMS/Pt) that could load a variety of functional materials, including drug molecules and nanoparticles, through channels of different sizes (Fig. 4C).[114] Doxorubicin (DOX) and heparinfolate (HF) nanoparticles were loaded into mesopores and macropores as anticancer drugs. Asymmetrically loaded Pt nanoparticles of a specific size in the macroporous structure were used as a power source for MMS/Pt by absorbing NIR. The penetration depth of nanomotors in three-dimensional (3D) multicellular tumor spheroids (MTSs) was about 110 μm under NIR irradiation compared to 60 μm for passive nanoparticles. *In vivo* experiments showed that the fluorescence intensity of MMS/Pt/HF/DOX in the tumor interior region under NIR irradiation was 1.8 times that of the non-NIR irradiation group. These results showed that the motion effect of nanomotors could promote the penetration of drugs into the tumor.

Single-atom catalysts have good stability over a wide temperature range, high ionic strength, and a wide pH environment.[149] Many single-atom catalysts are significantly more active in weakly acidic environments than in neutral environments, showing promising potential in tumor therapy.[150] However, due to the limited penetration capacity of the tumor, the efficacy of the single-atom catalyst will be reduced.[151] Recently, Xing *et al.* designed mesoporous carbon nanomotors coordinated with single-atom copper (Cu-JMPNs) (Fig. 4D).[25] Firstly, copper-doped jellyfish-like polydopamine nanoparticles were synthesized, and then inorganic silica shells were coated on Cu^{2+}-JMPN as nanoscaffolders. The copper single-atom could catalyze the conversion of H_2O_2 into toxic $^{\bullet}OH$ for chemokinetic therapy (CDT). Because the Cu-JMCNs had the same asymmetric structure as jellyfish and photothermal characteristics, and implemented Cu-JMCN self-thermophoresis triggered by NIR, the uptake and penetration of 3D tumor cells were significantly improved. *In vivo* experiments showed that single-atom Cu combined with CDT and NIR light could achieve a tumor inhibition rate of more than 85%.

Recently, inspired by space rockets, Zhang *et al.* designed nanorockets (NRs) that could achieve a two-stage conversion of light-to-heat-to-chemical energy (Fig. 4E).[115] First, the semiconducting polymer (SP) nanoparticles that can absorb NIR were synthesized to drive the nanomotor movement and generate heat to ablate the tumors. Then, pendant acyl azide underwent the thermo-driven Curtius rearrangement for robustly releasing nitrogen. In the PBS buffer, the corresponding average speeds of the nanorockets in response to 3 s irradiation could be accelerated from 21.5 to 63.9 μm s^{-1}. The average velocities of the nanorockets within 3 s could reach 15.8 μm s^{-1} at 37 °C and without NIR irradiation. In addition, the nanorockets could penetrate tumor vascular membranes, ECM, and cancer cell membranes sequentially under NIR irradiation, significantly improving tumor accumulation, tumor penetration, and cell uptake.

3.2.2 Bacterial biofilm barrier. Bacterial infection has become a great threat to human life and health, and the resistance of bacteria to antibiotics is a key issue in the treatment of bacterial infections.[152,153] Among them, the formation of bacterial biofilms is one of the key reasons for antibiotic resistance in various bacterial infections. Biofilms are multicellular three-dimensional microbial communities wrapped in self-produced exopolymer substances.[154] Destroying the physical integrity of biofilms is the most effective way to overcome bacterial biofilms. In order to eradicate bacterial biofilms, antibiotics and disinfectants usually need to be used 1000 times more than floating bacteria.[155] When the biofilm becomes incomplete, the bacteria will revert to a floating state and become more sensitive to host defenses and antimicrobials.[156,157] However, it is a huge challenge to completely destroy the biofilm to solve the problem of penetration depth and combat bacterial biofilm infection. At present, MMNs have been successfully applied in the fields of bacterial detection and biofilm removal because of their excellent motion performance.[158,159]

Boisen *et al.* designed a self-propelled mesoporous SiO_2/Au nanomotor driven by NIR light for the first time to eradicate *Pseudomonas aeruginosa* (*P. aeruginosa*) biofilms (Fig. 5A).[160] The MSNs were selected as the carrier of the nanoplatform and Au was unsymmetrically sputtered on the surface of the MSNs to prepare an asymmetric structure

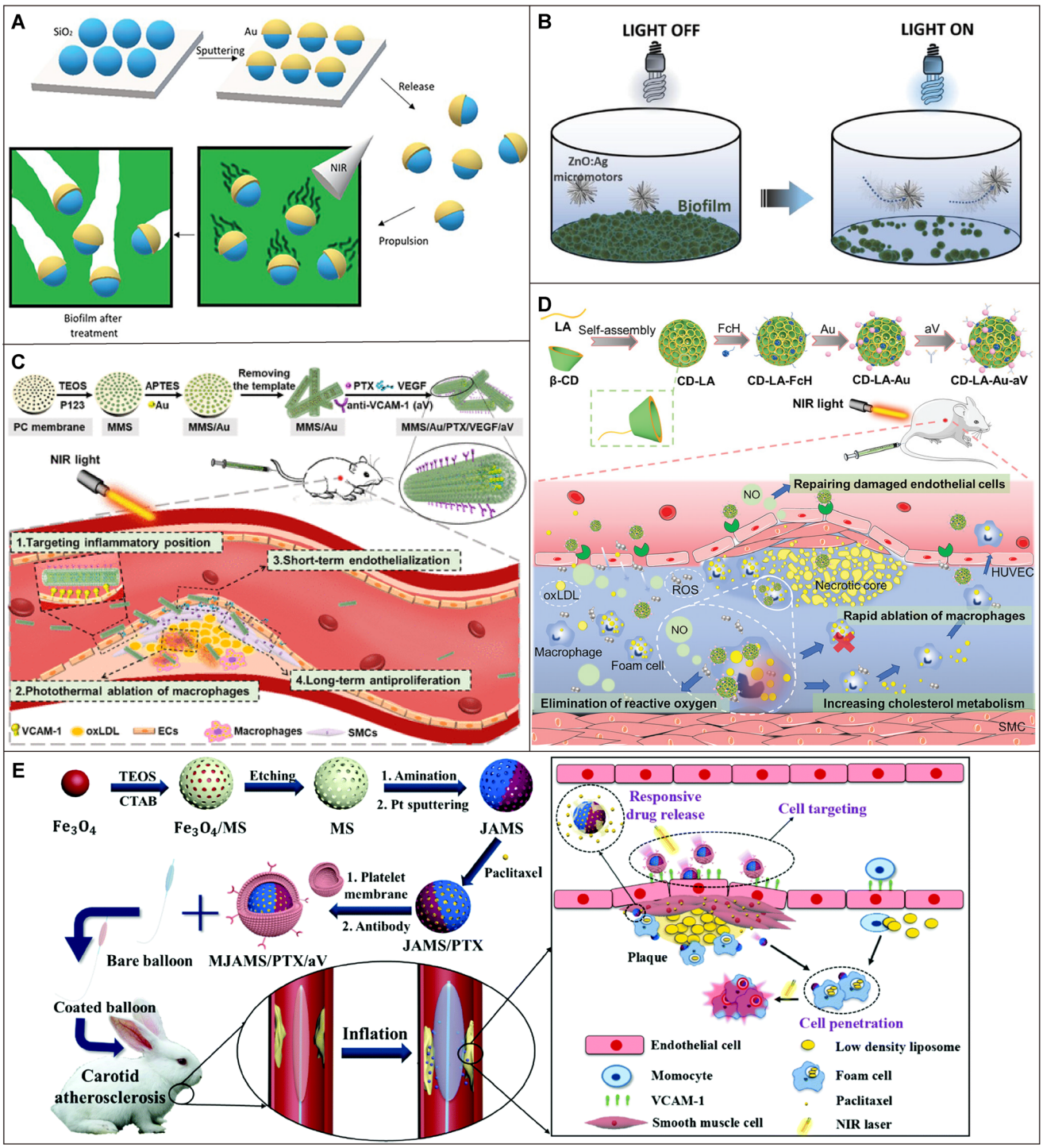

Fig. 5 Application of MNMs in penetrating the disease-associated barrier. (A) Schematic illustration of the fabrication of SiO_2/Au nanomotors, propulsion under an NIR irradiation light source, and biofilm eradication. Reproduced with permission.[160] Copyright 2023, Wiley-VCH GmbH. (B) Schematic illustration of self-propelled ZnO : Ag micromotors for bacterial biofilm eradication in water. Reproduced with permission.[116] Copyright 2021, Wiley-VCH GmbH. (C) Schematic illustration of micromotor preparation and its application in the treatment of atherosclerosis. Reproduced with permission.[66] Copyright 2020, American Chemical Society. (D) Schematic illustration of the nanomotors with dual-mode propulsion preparation and their application in the treatment of atherosclerosis. Reproduced with permission.[118] Copyright 2022, Wiley-VCH GmbH. (E) Schematic illustration of the synthesis process of MJAMS/PTX/aV and the mechanism of MJAMS/PTX/aV encapsulated balloon treatment for atherosclerosis. Reproduced with permission.[119] Copyright 2020, The Royal Society of Chemistry.

(SiO_2/Au). The SiO_2/Au nanomotors were able to reach speeds of about 86 μm s^{-1} at a laser power of 57.5 mW, regardless of the wavelength chosen in the near-infrared region. In addition, just 3 min of NIR exposure was enough to reduce bacterial biomass by 71%, which showed great promise for the eradication of bacterial biofilms by MNMs.

Unlike light-driven motors or motors with lower propulsion capacity, few examples of ZnO-based micromotors have been reported in the literature. More importantly, there are no examples of ZnO combined with Ag using *in situ* doping methods. A light-driven ZnO : Ag self-propelled micromotor was proposed by Ussia *et al.* for removing biofilms from solid surfaces (Fig. 5B).[116] ZnO : Ag micromotors which had an asymmetric structure were synthesized by a hydrothermal method, and the presence of Ag could enhance the photocatalytic performance of ZnO. Under the irradiation of UV light, the photogenerated electrons in ZnO were transferred to the Ag component, leaving holes on the ZnO side. The photogenerated electrons could produce ROS with O_2 and H_2O_2, while the holes could oxidize H_2O or decompose H_2O_2 into O_2 and protons, thus driving the movement of the nanomotors. In the presence of 1% H_2O_2, the average velocity of the ZnO : Ag micromotor increased to 4.5 ± 0.8 μm s^{-1}. Notably, up to 80% of the bacterial biofilm was eradicated within 5 minutes, showing excellent biofilm resistance against *Pseudomonas aeruginosa* (*P. aeruginosa*) at a micromotor concentration of 1 μg mL^{-1}.

In addition, black-TiO_2 (B-TiO_2) nanotubes also have good photocatalytic ability and biocompatibility with Ag. Ussia *et al.* proposed the first light-driven self-walking tubular nanorobot based on B-TiO_2 modified with Ag nanoparticles (B-TiO_2/Ag).[117] B-TiO_2 has a wide absorption characteristic from the UV to NIR band, which can promote the nanorobots to move under UV light. In the presence of UV and low concentrations of hydrogen peroxide, the ion gradient generated on the B-TiO_2 surface established a local electric field that allowed the nanorobots to advance through a self-electrophoresis mechanism. At 0.1% H_2O_2, the maximum rotational and random motion speeds of nanorobots were 500 ± 173 rpm and 31 ± 11 μm s^{-1}, respectively. The nanorobots could remove 40% of the bacterial biofilm in 30 minutes under motion conditions.

3.2.3 Vascular plaque barrier. Cardiovascular disease is often associated with atherosclerosis (AS), which begins with damage to the endothelium of the blood vessels and is characterized by fatty plaque buildup in the subcutaneous space inside the blood vessels.[161,162] It has been reported that some nanomedicines are delivered to AS plaques by targeted modifications, but the binding between the drug and the plaque is affected due to vascular pulsation and blood scour.[163] In addition, deep penetration and improvement of the penetration efficiency of agents after reaching the plaque site still remain the main challenges.[119,164] Light-driven MNMs can effectively promote infiltration and aggregation at the plaque site and the ablation of inflammatory macrophages through the photothermal effect, which is expected to become a highly potential strategy for the treatment of this disease.

Based on this, Li *et al.* designed a NIR light-driven tubular mesoporous silica micromotor loaded with Au NPs to form MMS/Au, which could quickly target damaged blood vessels and release different drugs including large sizes of vascular endothelial growth factor (VEGF) and small sizes of the antiproliferative drug paclitaxel (PTX) (Fig. 5C).[66] When the power of NIR was 2.5 W cm^{-2}, the velocity of the micromotors was about 12.2 μm s^{-1}, which allowed them to promote their own penetration into the plaque site under NIR irradiation. The results of *in vivo* experiments showed that micromotors had a good therapeutic effect on atherosclerosis. This kind of micromotor technology with a complex porous structure will have more potential as a disease treatment platform.

NO can improve anti-atherosclerosis by improving endothelial function and reducing oxidative stress.[165] Inspired by this, Wu *et al.* covalently bonded L-arginine (LA) to β-cyclodextrin (β-CD), which had the ability to dissolve cholesterol, to construct NO-driven nanomotors (Fig. 5D).[118] Au NPs were covalently bonded to the nanomotor surface to provide an additional driving force through the photothermal conversion properties of Au (CD-LA-Au). The CD-LA-Au nanomotors were continuously active in the NIR laser and ROS environment, and the movement speed could reach 5–8 μm s^{-1}. *In vivo* therapeutic effects showed that the nanomotor with dual-mode propulsion reduced the aortic plaque area to 5.2% in mice and had a positive effect against atherosclerosis.

Drug-coated balloons (DCBs) are among the clinical methods to treat atherosclerosis.[166] However, this treatment still has the disadvantage of poor drug retention and penetration in the diseased region.[167] To solve this problem, Huang *et al.* designed a drug-loaded porous nanomotor for DCBs (Fig. 5E).[119] The aminated mesoporous silica (AMS) was first prepared, and Pt was sprayed onto the AMS side to form Janus AMS (JAMS). Then, PTX and a targeted anti-vascular cell adhesion molecule-1 (anti-VCAM-1) antibody were modified on the nanomotor surface (JAMS/PTX/aV). Finally, the nanomotors were coated with platelet membranes (MJAMA/PTX/aV) to reduce the premature release of drugs. The ability of the nanomotors to move under NIR light could promote their retention and penetration at the plaque site, and the heat generated could promote the ablation of macrophages. This provided more clues to effective DCBs for the treatment of atherosclerosis.

In this part, we mainly introduced the application of light-driven MNMs in overcoming the physiological and pathological barriers in recent years. The unique driving mechanism and beneficial permeability of light-driven MNMs make them have great application potential in diseases related to barriers, such as gastrointestinal diseases, cardiovascular and cerebrovascular diseases, and tumors. However, at present, there are still some problems in the application of MNMs to clinical disease treatment. To address these challenges, researchers are expected to develop novel light-driven MNMs.

4. Current challenges

Thanks to the prosperity of nanotechnology, various types of MNMs have been reported.[29,168,169] Among these MNMs, the elaborately designed light-driven MNMs may be controlled noninvasively with highly precise spatial and temporal resolution.[70] As an emerging research direction in recent years, light-driven MNMs have shown great application potential in the fields of environmental remediation,[170,171] cargo delivery,[107,172] biomedicine,[58,173] and so on. Meanwhile, the advantages offered by light-driven MNMs are accompanied by disadvantages and limitations that need to be carefully considered. The following points are mainly described: (1) precise control of the speed and direction of light-driven MNMs, (2) efficient deep tissue penetration of light-driven MNMs, and (3) potential thermal damage to biological tissues caused by self-thermophoretic MNMs.

4.1 Precise control of the speed and direction of light-driven MNMs

With the rapid development of light-driven MNMs and their wide range of biomedical applications, their motion control has attracted much attention in recent years.[174] Researchers can precisely control objects at the macro level, but it is not easy at the micro level.[56] First of all, due to technical limitations, artificial chips cannot be manufactured on a very small scale and inserted into them, and some traditional methods will not be suitable.[56,175,176] In addition, the complex physiological environment in the body also interferes with the precise control of light-driven MNMs. In order to complete some of the more challenging and complex *in vivo* tasks, precise motion control and manipulation of light-driven MNMs are essential. Therefore, the following are several potential solutions to achieve precise control of the speed and direction of motion.

Firstly, isotropic semiconductor MNMs with precise light-controlled motion speed and direction can be designed. For example, Chen *et al.* prepared anatase isotropic TiO_2 micromotors with a diameter of 1.2 μm and a refractive index of 2.7–0.15i.[177] The isotropic TiO_2 micromotors produced linear negative phototaxis due to limited UV penetration depth and resulted in asymmetric surface chemical reactions on TiO_2 microspheres, thereby inducing the O_2 concentration gradient generated by photocatalyzed H_2O_2 to propel MNMs. The directionality of the motion of the developed TiO_2 micromotors was not disturbed by their rotational Brownian diffusion or local flows but was always in the direction of irradiated light. Similar to the phototaxis of microorganisms, the speed of motion could be fleetly and precisely controlled by adjusting the intensity of incident light.

Secondly, the light-driven method can be combined with other external field-driven methods, such as opto-magnetic-driven MNMs, and the combination of magnetic fields and lights can achieve precise orientation, as magnetic fields may still work effectively even after deep penetration. For instance, Guo *et al.* demonstrated that phototaxis miniature motor assembly isotropic magnetic bead@TiO_2 core–shell-structured micromotors (MB@TiO_2 MMs) aggregate as dynamic lines and have the ability to manipulate large cargos over a wide range.[178] By applying UV and static magnetic fields, the photocatalytic shell and the magnetic core of an isotropic micromotor can flock in line formations with controlled velocities and directions for microengineering and pathogen/toxin elimination. Li *et al.* developed swarming responsive photonic nanorobots (RPNRs) consisting of nanochains of periodically aligned Fe_3O_4 nanoparticles.[179] They could actively navigate in complex environments and instantly convert the physicochemical conditions of the microenvironment into visual color mapping signals, further guiding local photothermal therapy. Therefore, by combining with other external fields, the limitations of single light-driven MNMs in precise controlled motion can be overcome so that the light-driven MNMs can play a more excellent role in the diagnosis and treatment of diseases.

Last but not least, by combining MNMs with fluorescence, fluorescent MNMs with unique advantages have been developed. Specifically, fluorescence endows MNMs with fluorescent trackability, environmental sensitivity, and chemo-/photon-induced cytotoxicity *in vitro* or *in vivo*, while MNMs endow fluorescent substances with mobility, external navigation, and motile targets in complex biological environments.[180] As a result, functional fluorescent MNMs offer great potential for precise and controlled delivery of active drugs. Servant *et al.* reported artificial bacterial flagella (ABF) microrobots functionalized with a near-infrared fluorescent material (NIR-797).[181] Magnetic metal nickel implemented the wireless control of the ABF microrobot with an average speed of 70.4 μm s^{-1}. Due to the long-wave emission of the NIR-797 fluorophore, ABF whole-body fluorescent imaging could be done to realize the precise control of living body diagnosis and treatment. Thus, by combining with fluorescence to design fluorescent MNMs, after tracing the location of the nanomotor in the body, the fate of the nanomotor *in vivo* is accurately regulated by the laser with high spatiotemporal resolution.

4.2 Efficient deep tissue penetration of light-driven MNMs

The limited deep tissue penetration of nanoparticles *in vivo* remains a formidable challenge to their therapeutic efficacy.[182] Light-driven MNMs have excellent autonomous movement ability, showing great potential to cross deep tissues and efficiently perform *in vivo* tasks.[183] However, the selection of different light sources and insufficient driving force may affect the tissue penetration performance of light-driven MNMs. The following method may provide inspiration for efficient tissue penetration of light-driven MNMs.

For one thing, the wavelength of light used to drive the MNMs needs to be considered. The sources of light mainly include UV light, VIS light, and NIR light. UV can cause additional damage to organisms and VIS light has poor tissue penetration, hence, both are not suitable for widespread application *in vivo*. NIR light has good biological safety and high tissue penetration, which makes it more suitable for deep

tissue penetration applications.[184,185] Besides, appropriate light sources are selected according to different parts of the organism. (1) Irradiating light-responsive MNMs with NIR-I/NIR-II wavelengths have been used to penetrate deep tissue regions for excellent disease treatment. For example, Ji *et al.* prepared a NIR-I-propelled parachute-like nanomotor loaded with miconazole nitrate (PNM-MN) to enhance transdermal drug delivery for synergistic antifungal therapy.[112] Wang *et al.* developed NIR-II light-driven asymmetric hydrogel nanomotors with encapsulated DOX (AHNM-DOX), which facilitated deep tissue penetration and enhanced *in vivo* immunochemotherapy.[183] (2) Optical fiber can be selected for the diagnosis and treatment of gastrointestinal, respiratory and other luminal diseases. Hou *et al.* reported a swallowable X-ray dosimeter (containing an optical fiber) for the simultaneous real-time monitoring of the absolute absorbed radiation dose and the changes in pH and temperature.[186] Ran *et al.* utilized functional optical fibers to realize an *in vivo* endoscopic cancer sensing and therapy ensemble.[187] The above examples provide a solution for the diagnosis and treatment of intracavitary diseases with light-driven MNMs.

For another thing, sufficient driving force is beneficial for light-driven MNMs to traverse deep tissues and perform *in vivo* tasks. Dual-driven MNMs have more abundant driving force compared with single light-driven MNMs. Of note, the large number of bubbles produced by single bubble-driven MNMs is potentially harmful to normal tissues in the body. Thus, efforts can be made to design dual-driven MNMs with combined photothermal and photoinduced gas actuation. While obtaining sufficient driving force, the controlled release of gas can be achieved by adjusting the direction, intensity and irradiation time of the incident light. For example, Zhang *et al.* elaborately engineered a carrier-free self-assembled nanomotor (T-BD NAs) consisting of a photothermal photosensitizer and a photothermal activable NO donor.[188] The concentration of NO produced by NIR light irradiation of T-BD NAs depends on the concentration of BNN6 and the magnitude of the laser radiation power. More interestingly, NO generation from T-BD NAs demonstrated regular off–on variations along with the laser irradiation switch, suggesting a controllable NO generation feature of laser irradiation T-BD NAs.

Some donor substances can release gas signal molecules such as O_2,[189] H_2,[190] NO,[191–193] and H_2S[194] under light stimulation. Some of these gas members have the properties of weakening physiological and pathological barriers. For example, NO can reduce the integrity of the endothelial cell barrier reversibly.[195] Kim *et al.* showed NO-releasing *N,N′*-di-*sec*-butyl-*N,N′*-dinitroso-1,4-phenylenediamine (BNN6) and piezoelectric barium titanate nanoparticles (BTNPs) coated with polydopamine (pDA).[196] The release of NO temporarily disrupts the tight junctions in the BBB, allowing the nanoparticles to accumulate in the brain parenchyma. Moreover, several gas signaling molecules have been shown to have some specific therapeutic effects. For example, H_2 has anti-inflammatory, anti-reactive oxygen species, and anti-cancer physiological effects.[197] NO has a central role in signaling pathways involved in numerous physiological processes (*e.g.*, vasodilation, neurotransmission, inflammation, apoptosis, and tumor growth).[198] H_2S is recognized as an endogenous physiological regulator in a variety of mammalian cells and tissues.[199] Therefore, MNMs with combined photothermal and photoinduced gas propulsion can not only provide sufficient driving force but also produce gas signaling molecules with the physiological and pathological barrier weakening properties, synergistically exerting excellent ability of penetration into the deep tissue barrier and therapeutic effects on diseases. At the same time, efforts can be made to design light-driven MNMs that can be precisely controlled *in situ* to produce gas molecules to avoid potential damage to normal tissues.

4.3 Potential thermal damage caused by light-induced thermophoretic MNMs

Light-induced thermophoretic MNMs require high-intensity light to promote efficient locomotion. The high heat generated by the strong absorption of light by light-driven MNMs plays an excellent role in the treatment of some special diseases. For example, Fu *et al.* engineered test tube-shaped Au–Cu micromotors (MMs), where MMs can be driven under NIR irradiation and aggregate into a swarm.[200] The high temperature of 45.5 °C in the swarm center could be employed for photothermal therapy and tumor cell eradication. Ni *et al.* reported that NIR drives pure organic Janus nanoparticles (Janus-like NPs).[210] This strategy of enhancing PTT by pure organic Janus-like NPs not only promotes compact J-type aggregation but also enables the cascade photothermal–thermophoresis enhanced photothermal effect. However, it is also worth noting that NIR irradiation tends to cause an increase in the temperature of the living body, which may lead to changes in the biological environment and damage to normal cells or tissues.

Given this limitation, MNMs can be more efficiently gathered at the lesion site through active targeting, and NIR with high spatiotemporal resolution can illuminate the lesion site, thus reducing the damage to surrounding normal tissues. Feng *et al.* reported a COF-based biomimetic nanomotor of mPPy@COF-Por consisting of the PPy core, the porphyrin-COF shell, and HCT116 cancer cell membrane coating.[201] Under NIR light irradiation, cancer cell membrane camouflage nanomotors could actively target and identify cancer cells. This multifunctional integration made the COF-based nanomotor a powerful nanoagent for cancer therapy, and successfully achieved a combined photothermal/photodynamic therapy effect guided by high infrared thermal imaging/photoacoustic imaging/fluorescence three-modality imaging in HCT116 tumor cells. Besides, *in situ* polymerization of light-driven MNMs and photothermal conversion nanoparticles at focal sites could increase the contact area and accuracy of photothermal treatment and improve the efficiency of photothermal conversion. Li *et al.* presented a strategy to synergize a light-driven micromotor swarm with polydopamine for photothermal therapy in the physiological environment containing dopamine and GL261 mouse glioma cells.[202] The combination

of the wirelessly controlled micromotor swarm with *in situ* polymerized dopamine opens up new possibilities to overcome the limitations of inadequate NIR penetration and accidental damage to healthy tissues.

5. Conclusions and outlook

In spite of the great promise of targeted delivery systems for precision medicine applications, it is still difficult to meet many biomedical challenges (*e.g.*, clinical translation, biosafety, *etc.*), and newly developed light-driven MNMs provide new opportunities for this. First reported in the 1980s,[203] light-driven MNMs have become more and more widely known in recent years as rising stars in the field of MNMs due to their good biocompatibility,[95,197] easy access to driving forces (UV light,[107,204,205] NIR light,[74,206,207] and VIS light[174,208,209]), simple and efficient optical programming and control ability, and great flexibility.

This study provided an overview of the current applications of light-driven MNMs in biomedicine. First of all, the classification and mechanism of light-driven MNMs were introduced briefly. Subsequently, the applications of light-driven MNMs in overcoming physiological and pathological barriers for biomedical applications in the past five years were highlighted. For one thing, the ability of light-driven MNMs to break the inherent barriers of the body was introduced, including enhancing penetration into skin tissue, overcoming the mucus barrier, moving against blood flow, crossing the blood–brain barrier, *etc.* In addition, from the perspective of fighting against the disease matrix barrier: (1) light-driven MNMs can greatly penetrate the tumor tissue and exert excellent cancer therapeutic effects. (2) Light-driven MNMs can effectively promote infiltration and aggregation at the plaque site and the ablation of inflammatory macrophages through the photothermal effect, which is expected to become a highly potential strategy for the treatment of this disease. (3) Light-driven MNMs can be used to destroy bacterial biofilms, effectively eliminate bacteria, and enhance drug efficacy. In a word, due to the contact-free regulation and adjustable energy input of light-driven MNMs, as well as their excellent spatial and temporal resolution, they have performed several multifunctional tasks, including transporting cargo to specific locations in a precise and selective manner and overcoming physiological/pathological barriers to achieve excellent disease treatment effects. However, the clinical disease treatment of light-driven MNMs still faces some difficulties (such as biological safety, accurate localization of diseased cells, *etc.*), which requires the unremitting efforts of researchers. Despite facing several issues, light-driven MNMs have tremendous advantages in the biomedical domain compared to current passive targeted drug delivery.

To this end, we provide the following proposals for the further development of light-driven MNMs. Firstly, biocompatibility is the basis for the application of light-driven MNMs in biomedical fields. Biocompatibility and biodegradability should be of particular concern to avoid potential damage to normal tissues. Given the special environment of living organisms, combining cellular derivatives with biocompatible NIR light-responsive materials would be a possible strategy to improve the biocompatibility of light-driven MNMs. In addition, light-driven MNMs used to achieve precise localization of diseased cells, autonomous navigation of movement and parking are essential for their *in vivo* diagnosis and therapy. Therefore, efforts can be devoted to designing intelligent light-driven MNMs, which combine biosensing elements and driving forces generated by NIR light irradiation, to realize autonomous movement, rapid positioning and the release of cargo by sensing changes in the external environment through micro-sensing elements. Taken together, further development of light-driven MNMs should strive to combine high efficiency, versatility, and biocompatibility for more effective use in targeted therapy, *in situ* imaging, and *in vivo* diagnostics, especially in hard-to-reach locations. We have sufficient reasons to believe that in the near future, light-driven MNMs will make epoch-making progress in the field of precision medicine.

Author contributions

X. Zeng: methodology and writing – original draft. M. Yang: investigation and writing – original draft. H. Liu: formal analysis and writing – original draft. Z. Zhang: supervision and funding acquisition. Y. Hu: data curation and resources. J. Shi: conceptualization and project administration. Z. H. Wang: writing – review & editing and visualization.

Conflicts of interest

There are no conflicts of interest to declare.

Acknowledgements

This work was supported by the National Natural Science Foundation of China (no. 82222067, 82102936, 82172762, 31900991, 82073787, and 82073395), the China Postdoctoral Science Foundation (no. 2021M702959), and the Outstanding Youth Foundation of Henan Province Henan (no. 222300420020).

References

1 H. Ibrahim, *QJM*, 2020, **113**, hcaa060.008.
2 J. Shin, N. Kang, B. Kim, H. Hong, L. Yu, J. Kim, H. Kang and J. S. Kim, *Chem. Soc. Rev.*, 2023, **52**, 4488–4514.
3 I. Rezic, *Polymers*, 2022, **14**, 4961.
4 W. C. W. Chan, *Acc. Chem. Res.*, 2017, **50**, 627–632.
5 M. Chang, C. Dong, H. Huang, L. Ding, W. Feng and Y. Chen, *Adv. Funct. Mater.*, 2022, **32**, 2204791.

6 S. Kansız and Y. M. Elçin, *Adv. Colloid Interface Sci.*, 2023, **317**, 102930.
7 M. Moharramnejad, R. E. Malekshah, A. Ehsani, S. Gharanli, M. Shahi, S. A. Alvan, Z. Salariyeh, M. N. Azadani, J. Haribabu, Z. S. Basmenj, A. Khaleghian, H. Saremi, Z. Hassani and E. Momeni, *Adv. Colloid Interface Sci.*, 2023, **316**, 102908.
8 N. Iturrioz-Rodríguez, N. Sampron and A. Matheu, *Theranostics*, 2023, **13**, 2734–2756.
9 F. Pinelli, G. Perale and F. Rossi, *Gels*, 2020, **16**, 6–22.
10 X. Zhou, X. Huang, B. Wang, L. Tan, Y. Zhang and Y. Jiao, *Chem. Eng. J.*, 2021, **408**, 127897.
11 R. Sun, J. Xiang, Q. Zhou, Y. Piao, J. Tang, S. Shao, Z. Zhou, Y. H. Bae and Y. Shen, *Adv. Drug Delivery Rev.*, 2022, **191**, 114614.
12 S. Wilhelm, A. J. Tavares, Q. Dai, S. Ohta, J. Audet, H. F. Dvorak and W. C. W. Chan, *Nat. Rev. Mater.*, 2016, **1**, 16014.
13 C. Gao, Y. Wang, Z. Ye, Z. Lin, X. Ma and Q. He, *Adv. Mater.*, 2020, **33**, 2000512.
14 H. Li, F. Peng, X. Yan, C. Mao, X. Ma, D. A. Wilson, Q. He and Y. Tu, *Acta Pharm. Sin. B*, 2023, **13**, 517–541.
15 M. Luo, Y. Feng, T. Wang and J. Guan, *Adv. Funct. Mater.*, 2018, **28**, 1706100.
16 W. Liu, Y. Liu, H. Li, H. Nie, M. Tian and W. Long, *Adv. Funct. Mater.*, 2023, **33**, 2212452.
17 H. Choi, J. Yi, S. H. Cho and S. K. Hahn, *Biomaterials*, 2021, **279**, 121201.
18 M. Fernández-Medina, M. A. Ramos–Docampo, O. Hovorka, V. Salgueiriño and B. Städler, *Adv. Funct. Mater.*, 2020, **30**, 1908283.
19 T. Liu, L. Xie, C. H. Price, J. Liu, Q. He and B. Kong, *Chem. Soc. Rev.*, 2022, **51**, 10083–10119.
20 J. Ou, K. Liu, J. Jiang, D. A. Wilson, L. Liu, F. Wang, S. Wang, Y. Tu and F. Peng, *Small*, 2020, **16**, e1906184.
21 J. Meng, K. Wei, S. Xie, Z. Zhang, P. Ran, P. Zhang and X. Li, *J. Controlled Release*, 2023, **357**, 342–355.
22 P. Diez, E. Lucena-Sanchez, A. Escudero, A. Llopis-Lorente, R. Villalonga and R. Martinez-Manez, *ACS Nano*, 2021, **15**, 4467–4480.
23 B. Esteban-Fernández de Ávila, A. Martín, F. Soto, M. A. Lopez-Ramirez, S. Campuzano, G. M. Vásquez-Machado, W. Gao, L. Zhang and J. Wang, *ACS Nano*, 2015, **9**, 6756–6764.
24 B. Wang, K. F. Chan, K. Yuan, Q. Wang, X. Xia, L. Yang, H. Ko, Y.-X. J. Wang, J. J. Y. Sung, P. W. Y. Chiu and L. Zhang, *Sci. Rob.*, 2021, **6**, eabd2813.
25 W. Wang, E. Ma, P. Tao, X. Zhou, Y. Xing, L. Chen, Y. Zhang, J. Li, K. Xu, H. Wang and S. Zheng, *J. Mater. Sci. Technol.*, 2023, **148**, 171–185.
26 Y. Xing, J. Xiu, M. Zhou, T. Xu, M. Zhang, H. Li, X. Li, X. Du, T. Ma and X. Zhang, *ACS Nano*, 2023, **17**, 6789–6799.
27 J. Li, B. Esteban-Fernández de Ávila, W. Gao, L. Zhang and J. Wang, *Sci. Rob.*, 2017, **2**, eaam6431.
28 W. Xu, H. Qin, H. Tian, L. Liu, J. Gao, F. Peng and Y. Tu, *Appl. Mater. Today*, 2022, **27**, 101482.
29 X. Chang, Y. Feng, B. Guo, D. Zhou and L. Li, *Nanoscale*, 2022, **14**, 219–238.
30 R. Lin, W. Yu, X. Chen and H. Gao, *Adv. Healthcare Mater.*, 2021, **10**, e2001212.
31 J. Shao, S. Cao, H. Che, M. T. De Martino, H. Wu, L. Abdelmohsen and J. C. M. van Hest, *J. Am. Chem. Soc.*, 2022, **144**, 11246–11252.
32 Z. Wang, Y. Yan, C. Li, Y. Yu, S. Cheng, S. Chen, X. Zhu, L. Sun, W. Tao, J. Liu and F. Wang, *ACS Nano*, 2022, **16**, 9019–9030.
33 Y. Wu, Z. Song, G. Deng, K. Jiang, H. Wang, X. Zhang and H. Han, *Small*, 2021, **17**, e2006877.
34 X. Fang, H. Ye, K. Shi, K. Wang, Y. Huang, X. Zhang and J. Pan, *ACS Biomater. Sci. Eng.*, 2023, **9**, 4302–4310.
35 J. Yu, Y. Li, A. Yan, Y. Gao, F. Xiao, Z. Xu, J. Xu, S. Yu, J. Liu and H. Sun, *Adv. Sci.*, 2023, **14**, e2301919.
36 J. Zheng, W. Wang, X. Gao, S. Zhao, W. Chen, J. Li and Y. N. Liu, *Small*, 2022, **18**, e2205252.
37 Z. Liu, S. Liu, X. Zhao, C. Xue, Y. Liu and Q. Shuai, *Int. J. Biol. Macromol.*, 2023, **240**, 124486.
38 H. Tian, J. Ou, Y. Wang, J. Sun, J. Gao, Y. Ye, R. Zhang, B. Chen, F. Wang, W. Huang, H. Li, L. Liu, C. Shao, Z. Xu, F. Peng and Y. Tu, *Acta Pharm. Sin. B*, 2023, **13**, 2211–3835.
39 Z. Yang, L. Wang, Z. Gao, X. Hao, M. Luo, Z. Yu and J. Guan, *ACS Nano*, 2023, **17**, 6023–6035.
40 D. Fu, Y. Ye, C. Gao, D. Xie and F. Peng, *ChemNanoMat*, 2022, **8**, e202200152.
41 Y. Feng, M. An, Y. Liu, M. T. Sarwar and H. Yang, *Adv. Funct. Mater.*, 2022, **33**, 1616–3028.
42 S. Naeem, F. Naeem, J. Mujtaba, A. K. Shukla, S. Mitra, G. Huang, L. Gulina, P. Rudakovskaya, J. Cui, V. Tolstoy, D. Gorin, Y. Mei, A. A. Solovev and K. K. Dey, *Micromachines*, 2021, **12**, 1251.
43 G. Tezel, S. S. Timur, F. Kuralay, R. N. Gursoy, K. Ulubayram, L. Oner and H. Eroglu, *J. Drug Targeting*, 2021, **29**, 29–45.
44 H. Sipova-Jungova, D. Andren, S. Jones and M. Kall, *Chem. Rev.*, 2020, **120**, 269–287.
45 S. Zhang, X. Liu, Y. Hao, H. Yang, W. Zhao, C. Mao and S. Ma, *J. Colloid Interface Sci.*, 2023, **650**, 67–80.
46 X. Zhang, C. Liu, Y. Lyu, N. Xing, J. Li, K. Song and X. Yan, *J. Colloid Interface Sci.*, 2023, **648**, 457–472.
47 F. Qin, Y. Zhang and F. Peng, *ChemNanoMat*, 2021, **7**, 415–428.
48 Y. Zhu, Y. Song, Z. Cao, L. Dong, Y. Lu, X. Yang and J. Wang, *Adv. Funct. Mater.*, 2021, **31**, 2103655.
49 Y. Zhu, Y. Song, Z. Cao, L. Dong, S. Shen, Y. Lu and X. Yang, *Adv. Sci.*, 2023, **10**, e2204793.
50 J. Li, C. C. Mayorga-Martinez, C. D. Ohl and M. Pumera, *Adv. Funct. Mater.*, 2021, **32**, 2102265.
51 J. Ye, Q. Fu, L. Liu, L. Chen, X. Zhang, Q. Li, Z. Li, L. Su, R. Zhu, J. Song and H. Yang, *Sci. China: Chem.*, 2021, **64**, 2218–2229.

52 X. Sun, M. Wei, X. Pang, L. Lin, Q. Gao, L. Su, T. Liu, Y. Yao, J. Song, W. Wang and X. Yan, *Adv. Funct. Mater.*, 2023, **12**, 2214619.
53 J. Guo and D. Fan, *ChemNanoMat*, 2018, **4**, 1023–1038.
54 J. Meng, P. Zhang, Q. Liu, P. Ran, S. Xie, J. Wei and X. Li, *Acta Biomater.*, 2023, **162**, 20–31.
55 L. Zhang, Y. Qiu, W.-G. Liu, H. Chen, D. Shen, B. Song, K. Cai, H. Wu, Y. Jiao, Y. Feng, J. S. W. Seale, C. Pezzato, J. Tian, Y. Tan, X.-Y. Chen, Q.-H. Guo, C. L. Stern, D. Philp, R. D. Astumian, W. A. Goddard and J. F. Stoddart, *Nature*, 2023, **613**, 280–286.
56 Z. Zhan, F. Wei, J. Zheng, W. Yang, J. Luo and L. Yao, *Nanotechnol. Rev.*, 2018, **7**, 555–581.
57 C. Liu, J. Huang, T. Xu and X. Zhang, *Mikrochim. Acta*, 2022, **189**, 116–189.
58 J. Wang, Z. Xiong, J. Zheng, X. Zhan and J. Tang, *Acc. Chem. Res.*, 2018, **51**, 1957–1965.
59 K. Yuan, J. Bujalance-Fernandez, B. Jurado-Sanchez and A. Escarpa, *Mikrochim. Acta*, 2020, **187**, 581–768.
60 Z. H. Wang, W. Huang, S. Zhang, M. Chu, N. Yin, C. Zhu, Z. Zhang, J. Shi and J. Liu, *Adv. Funct. Mater.*, 2023, **33**, 2212013.
61 W. Liu, W. Wang, X. Dong and Y. Sun, *ACS Appl. Mater. Interfaces*, 2020, **12**, 12618–12628.
62 M. Pacheco, B. Jurado-Sanchez and A. Escarpa, *Nanoscale*, 2021, **13**, 17106–17115.
63 L. Liu, S. Li, K. Yang, Z. Chen, Q. Li, L. Zheng, Z. Wu, X. Zhang, L. Su, Y. Wu and J. Song, *Nano Lett.*, 2023, **23**, 3929–3938.
64 Y. Liu, Y. Zhang, J. Wang, H. Yang, J. Zhou and W. Zhao, *Bioconjugate Chem.*, 2022, **33**, 726–735.
65 Y. Zhang, K. Zhang, H. Yang, Y. Hao, J. Zhang, W. Zhao, S. Zhang, S. Ma and C. Mao, *ACS Appl. Mater. Interfaces*, 2023, **15**, 14009–14110.
66 X. Li, R. Wu, H. Chen, T. Li, H. Jiang, X. Xu, X. Tang, M. Wan, C. Mao and D. Shi, *ACS Appl. Mater. Interfaces*, 2021, **13**, 30930–30940.
67 D. Rojas, M. Kuthanova, K. Dolezelikova and M. Pumera, *NPG Asia Mater.*, 2022, **14**, 1884–4057.
68 R. Lin, W. Yu, X. Chen and H. Gao, *Adv. Healthcare Mater.*, 2021, **10**, e2001212.
69 C. Liu, J. Huang, T. Xu and X. Zhang, *Mikrochim. Acta*, 2022, **189**, 116.
70 L. Xu, F. Mou, H. Gong, M. Luo and J. Guan, *Chem. Soc. Rev.*, 2017, **46**, 6905–6926.
71 M. Xuan, Z. Wu, J. Shao, L. Dai, T. Si and Q. He, *J. Am. Chem. Soc.*, 2016, **138**, 6492–6497.
72 P. Mayorga-Burrezo, C. C. Mayorga-Martinez and M. Pumera, *Adv. Funct. Mater.*, 2021, **32**, 2106699.
73 E. Gruber, A. M. Kabylda, M. B. Nielsen, A. P. Rasmussen, R. Teiwes, P. A. Kusochek, A. V. Bochenkova and L. H. Andersen, *J. Am. Chem. Soc.*, 2022, **144**, 69–73.
74 T. Maric, A. Lovind, Z. Zhang, J. Geng and A. Boisen, *Adv. Healthcare Mater.*, 2023, **12**, e2203018.
75 M. Liu, L. Chen, Z. Zhao, M. Liu, T. Zhao, Y. Ma, Q. Zhou, Y. S. Ibrahim, A. A. Elzatahry, X. Li and D. Zhao, *J. Am. Chem. Soc.*, 2022, **144**, 3892–3901.
76 J. Wang, Z. Xiong, M. Liu, X.-m. Li, J. Zheng, X. Zhan, W. Ding, J. Chen, X. Li, X. D. Li, S.-P. Feng and J. Tang, *ACS Nano*, 2020, **14**, 3272–3280.
77 X. Wang, L. Baraban, A. Nguyen, J. Ge, V. R. Misko, J. Tempere, F. Nori, P. Formanek, T. Huang, G. Cuniberti, J. Fassbender and D. Makarov, *Small*, 2018, **14**, e1803613.
78 Z. T. Shi, Y. X. Hu, Z. Hu, Q. Zhang, S. Y. Chen, M. Chen, J. J. Yu, G. Q. Yin, H. Sun, L. Xu, X. Li, B. L. Feringa, H. B. Yang, H. Tian and D. H. Qu, *J. Am. Chem. Soc.*, 2021, **143**, 442–452.
79 J. G. Moo, S. Presolski and M. Pumera, *ACS Nano*, 2016, **10**, 3543–3552.
80 K. Yuan, J. Bujalance-Fernandez, B. Jurado-Sanchez and A. Escarpa, *Mikrochim. Acta*, 2020, **187**, 581.
81 Z. Wu, T. Si, W. Gao, X. Lin, J. Wang and Q. He, *Small*, 2016, **12**, 577–582.
82 D. Mateo, J. L. Cerrillo, S. Durini and J. Gascon, *Chem. Soc. Rev.*, 2021, **50**, 2173–2210.
83 J. T. Kim, U. Choudhury, H. H. Jeong and P. Fischer, *Adv. Mater.*, 2017, **29**, 1701024.
84 P. P. Yang, Y. G. Zhai, G. B. Qi, Y. X. Lin, Q. Luo, Y. Yang, A. P. Xu, C. Yang, Y. S. Li, L. Wang and H. Wang, *Small*, 2016, **12**, 5423–5430.
85 T. Bickel, A. Majee and A. Wurger, *Phys. Rev. E: Stat., Nonlinear, Soft Matter Phys.*, 2013, **88**, 012301.
86 S. Zheng, Y. Wang, S. Pan, E. Ma, S. Jin, M. Jiao, W. Wang, J. Li, K. Xu and H. Wang, *Adv. Funct. Mater.*, 2021, **31**, 2100936.
87 S. Cao, J. Shao, H. Wu, S. Song, M. T. De Martino, I. A. B. Pijpers, H. Friedrich, L. Abdelmohsen, D. S. Williams and J. C. M. van Hest, *Nat. Commun.*, 2021, **12**, 2077.
88 X. Zhen, K. Pu and X. Jiang, *Small*, 2021, **17**, e2004723.
89 Y. Jiang and K. Pu, *Acc. Chem. Res.*, 2018, **51**, 1840–1849.
90 X. Huang, Y. Liu, A. Feng, X. Cheng, X. Xiong, Z. Wang, Z. He, J. Guo, S. Wang and X. Yan, *Small*, 2022, **18**, e2201525.
91 M. Chen, E. Ma, Y. Xing, H. Xu, L. Chen, Y. Wang, Y. Zhang, J. Li, H. Wang and S. Zheng, *ACS Sens.*, 2023, **8**, 757–766.
92 L. Gui, J. Huang, Y. Xing, Y. Li, J. Zou, Y. Zhu, X. Liang, X. Zhang, Q. Xu and X. Du, *Nano Res.*, 2023, **16**, 5108–5120.
93 Y. Li, F. Mou, C. Chen, M. You, Y. Yin, L. Xu and J. Guan, *RSC Adv.*, 2016, **6**, 10697–10703.
94 F. Mou, Y. Li, C. Chen, W. Li, Y. Yin, H. Ma and J. Guan, *Small*, 2015, **11**, 2564–2570.
95 K. Villa and M. Pumera, *Chem. Soc. Rev.*, 2019, **48**, 4966–4978.
96 F. Mou, L. Kong, C. Chen, Z. Chen, L. Xu and J. Guan, *Nanoscale*, 2016, **8**, 4976–4983.
97 R. Dong, Q. Zhang, W. Gao, A. Pei and B. Ren, *ACS Nano*, 2016, **10**, 839–844.

98 J. Wang, Z. Xiong, J. Zheng, X. Zhan and J. Tang, *Acc. Chem. Res.*, 2018, **51**, 1957–1965.
99 Q. Zhang, R. Dong, Y. Wu, W. Gao, Z. He and B. Ren, *ACS Appl. Mater. Interfaces*, 2017, **9**, 4674–4683.
100 G. Jackson, *Int. J. Opt.*, 2010, **16**, 1–16.
101 F. Ercole, T. P. Davis and R. A. Evans, *Polym. Chem.*, 2010, **1**, 37–54.
102 J. P. Abid, M. Frigoli, R. Pansu, J. Szeftel, J. Zyss, C. Larpent and S. Brasselet, *Langmuir*, 2011, **27**, 7967–7971.
103 W. Li, X. Wu, H. Qin, Z. Zhao and H. Liu, *Adv. Funct. Mater.*, 2016, **26**, 3164–3171.
104 A. A. Beharry and G. A. Woolley, *Chem. Soc. Rev.*, 2011, **40**, 4422–4437.
105 A. Kausar, H. Nagano, T. Ogata, T. Nonaka and S. Kurihara, *Angew. Chem., Int. Ed.*, 2009, **48**, 2144–2147.
106 Z. Ye, Y. Wang, S. Liu, D. Xu, W. Wang and X. Ma, *J. Am. Chem. Soc.*, 2021, **143**, 15063–15072.
107 X. Xiong, X. Huang, Y. Liu, A. Feng, Z. Wang, X. Cheng, Z. He, S. Wang, J. Guo and X. Yan, *Chem. Eng. J.*, 2022, **445**, 136576.
108 C. Gao, Y. Wang, Z. Ye, Z. Lin, X. Ma and Q. He, *Adv. Mater.*, 2021, **33**, e2000512.
109 Z. H. Wang, M. Chu, W. Huang, W. Liu, Z. Zhang, J. Shi and J. Liu, *Sci. Adv.*, 2022, **8**, eabn3917.
110 J. Shao, M. Abdelghani, G. Shen, S. Cao, D. S. Williams and J. C. M. van Hest, *ACS Nano*, 2018, **12**, 4877–4885.
111 F. Lin, Y. Shao, Y. Wu and Y. Zhang, *ACS Appl. Mater. Interfaces*, 2021, **13**, 3713–3721.
112 X. Ji, H. Yang, W. Liu, Y. Ma, J. Wu, X. Zong, P. Yuan, X. Chen, C. Yang, X. Li, H. Lin, W. Xue and J. Dai, *ACS Nano*, 2021, **15**, 14218–14228.
113 Z. Zhang, T. Xia, P. Ran, J. Wei, J. Meng, G. Zhang and X. Li, *Chem. Eng. J.*, 2023, **457**, 141226.
114 M. Wan, Q. Wang, X. Li, B. Xu, D. Fang, T. Li, Y. Yu, L. Fang, Y. Wang, M. Wang, F. Wang, C. Mao, J. Shen and J. Wei, *Angew. Chem., Int. Ed.*, 2020, **59**, 14458–14465.
115 A. Feng, X. Cheng, X. Huang, Y. Liu, Z. He, J. Zhao, H. Duan, Z. Shi, J. Guo, S. Wang and X. Yan, *Small*, 2023, **19**, e2206426.
116 M. Ussia, M. Urso, K. Dolezelikova, H. Michalkova, V. Adam and M. Pumera, *Adv. Funct. Mater.*, 2021, **31**, 2101178.
117 M. Ussia, M. Urso, S. Kment, T. Fialova, K. Klima, K. Dolezelikova and M. Pumera, *Small*, 2022, **18**, e2200708.
118 Z. Wu, R. Wu, X. Li, X. Wang, X. Tang, K. Tan, M. Wan, C. Mao, X. Xu, H. Jiang, J. Li, M. Zhou and D. Shi, *Small*, 2022, **18**, e2104120.
119 Y. Huang, T. Li, W. Gao, Q. Wang, X. Li, C. Mao, M. Zhou, M. Wan and J. Shen, *J. Mater. Chem. B*, 2020, **8**, 5765–5775.
120 Y. Lee, N. Kamada and J. J. Moon, *Adv. Drug Delivery Rev.*, 2021, **179**, 114021.
121 M. Boegh and H. M. Nielsen, *Basic Clin. Pharmacol. Toxicol.*, 2015, **116**, 179–186.
122 L. M. Ensign, R. Cone and J. Hanes, *Adv. Drug Delivery Rev.*, 2012, **64**, 557–570.
123 S. Zhang, C. Zhu, W. Huang, H. Liu, M. Yang, X. Zeng, Z. Zhang, J. Liu, J. Shi, Y. Hu, X. Shi and Z. H. Wang, *J. Controlled Release*, 2023, **360**, 514–527.
124 J. T. Huckaby and S. K. Lai, *Adv. Drug Delivery Rev.*, 2018, **124**, 125–139.
125 X. Murgia, B. Loretz, O. Hartwig, M. Hittinger and C. M. Lehr, *Adv. Drug Delivery Rev.*, 2018, **124**, 82–97.
126 K. Masamoto, R. Hoshikawa and H. Kawaguchi, *Curr. Top. Med. Chem.*, 2016, **8**, 2677–2684.
127 X. Zhan, J. Wang, Z. Xiong, X. Zhang, Y. Zhou, J. Zheng, J. Chen, S. P. Feng and J. Tang, *Nat. Commun.*, 2019, **10**, 3921.
128 J. L. D. Atkinson, R. E. Anderson and T. M. Sundt Jr, *Brain Res.*, 1990, **517**, 330–340.
129 Q. Wang and L. Zhang, *ACS Nano*, 2021, **15**, 149–174.
130 S. Seo, H. Kim, J. H. Sung, N. Choi, K. Lee and H. N. Kim, *Biomaterials*, 2020, **232**, 119732.
131 S. Ding, A. I. Khan, X. Cai, Y. Song, Z. Lyu, D. Du, P. Dutta and Y. Lin, *Mater. Today*, 2020, **37**, 112–125.
132 W. M. Pardridge, *Drug Discovery Today*, 2007, **12**, 54–61.
133 D. Wu, Q. Chen, X. Chen, F. Han, Z. Chen and Y. Wang, *Signal Transduction Targeted Ther.*, 2023, **8**, 217.
134 M. M. Patel and B. M. Patel, *CNS Drugs*, 2017, **31**, 109–133.
135 H. Chen, T. Li, Z. Liu, S. Tang, J. Tong, Y. Tao, Z. Zhao, N. Li, C. Mao, J. Shen and M. Wan, *Nat. Commun.*, 2023, **14**, 941.
136 K. Kwiecien, A. Zegar, J. Jung, P. Brzoza, M. Kwitniewski, U. Godlewska, B. Grygier, P. Kwiecinska, A. Morytko and J. Cichy, *Cytokine Growth Factor Rev.*, 2019, **49**, 70–84.
137 A. Tavakkoli, T. P. Johnston and A. Sahebkar, *Pharmacol. Ther.*, 2020, **208**, 107483.
138 K. Peng, L. K. Vora, I. A. Tekko, A. D. Permana, J. Dominguez-Robles, D. Ramadon, P. Chambers, H. O. McCarthy, E. Larraneta and R. F. Donnelly, *J. Controlled Release*, 2021, **339**, 361–380.
139 E. V. Lengert, E. E. Talnikova, V. V. Tuchin and Y. I. Svenskaya, *Skin Pharmacol. Physiol.*, 2020, **33**, 261–269.
140 B. Li, P. Ji, S. Y. Peng, P. Pan, D. W. Zheng, C. X. Li, Y. X. Sun and X. Z. Zhang, *Adv. Mater.*, 2020, **32**, e2000376.
141 G. Hong, A. L. Antaris and H. Dai, *Nat. Biomed. Eng.*, 2017, **1**, 1–22.
142 Z. Sun, T. Wang, J. Wang, J. Xu, T. Shen, T. Zhang, B. Zhang, S. Gao, C. Zhao, M. Yang, F. Sheng, J. Yu and Y. Hou, *J. Am. Chem. Soc.*, 2023, **145**, 11019–11032.
143 Q. Li, L. Liu, H. Huo, L. Su, Y. Wu, H. Lin, X. Ge, J. Mu, X. Zhang, L. Zheng and J. Song, *ACS Nano*, 2022, **16**, 7947–7960.
144 T. Wang, E. J. Cornel, C. Li and J. Du, *J. Controlled Release*, 2023, **353**, 350–365.
145 J. L. Au, B. Z. Yeung, M. G. Wientjes, Z. Lu and M. G. Wientjes, *Adv. Drug Delivery Rev.*, 2016, **97**, 280–301.

146 B. Ouyang, B. R. Kingston, W. Poon, Y. N. Zhang, Z. P. Lin, A. M. Syed, J. Couture-Senecal and W. C. W. Chan, *Mol. Pharm.*, 2022, **19**, 1917–1925.
147 X. Li, J. F. Lovell, J. Yoon and X. Chen, *Nat. Rev. Clin. Oncol.*, 2020, **17**, 657–674.
148 Y. Jiang, X. Pang, R. Liu, Q. Xiao, P. Wang, A. W. Leung, Y. Luan and C. Xu, *ACS Appl. Mater. Interfaces*, 2018, **10**, 31674–31685.
149 W. Ma, J. Mao, X. Yang, C. Pan, W. Chen, M. Wang, P. Yu, L. Mao and Y. Li, *Chem. Commun.*, 2018, **55**, 159–162.
150 X. Lu, S. Gao, H. Lin, L. Yu, Y. Han, P. Zhu, W. Bao, H. Yao, Y. Chen and J. Shi, *Adv. Mater.*, 2020, **32**, e2002246.
151 X. Lu, S. Gao, H. Lin and J. Shi, *Small*, 2021, **17**, e2004467.
152 M. Bassetti, T. Welte and R. G. Wunderink, *Crit. Care*, 2016, **20**, 19.
153 C. Pecoraro, D. Carbone, D. Deng, S. M. Cascioferro, P. Diana and E. Giovannetti, *Curr. Med. Chem.*, 2022, **29**, 4307–4310.
154 H. C. Flemming and J. Wingender, *Nat. Rev. Microbiol.*, 2010, **8**, 623–633.
155 S. Sugimoto, F. Sato, R. Miyakawa, A. Chiba, S. Onodera, S. Hori and Y. Mizunoe, *Sci. Rep.*, 2018, **8**, 2254.
156 R. A. G. da Silva, I. Afonina and K. A. Kline, *Curr. Opin. Microbiol.*, 2021, **63**, 117–125.
157 H. Ji, H. Hu, Q. Tang, X. Kang, X. Liu, L. Zhao, R. Jing, M. Wu, G. Li, X. Zhou, J. Liu, Q. Wang, H. Cong, L. Wu and Y. Qin, *J. Hazard. Mater.*, 2022, **436**, 129210.
158 V. Milosavljevic, L. Kosaristanova, K. Dolezelikova, V. Adam and M. Pumera, *Adv. Funct. Mater.*, 2022, **32**, 2112935.
159 L. Zhao, S. Xie, Y. Liu, Q. Liu, X. Song and X. Li, *Nanoscale*, 2019, **11**, 17831–17840.
160 T. Maric, A. Lovind, Z. Zhang, J. Geng and A. Boisen, *Adv. Healthcare Mater.*, 2023, **12**, e2203018.
161 S. Zhang, Y. Liu, Y. Cao, S. Zhang, J. Sun, Y. Wang, S. Song and H. Zhang, *Adv. Mater.*, 2022, **34**, e2110660.
162 A. Mallone, C. Stenger, A. Von Eckardstein, S. P. Hoerstrup and B. Weber, *Biomaterials*, 2018, **150**, 49–59.
163 Y. Wang, K. Zhang, X. Qin, T. Li, J. Qiu, T. Yin, J. Huang, S. McGinty, G. Pontrelli, J. Ren, Q. Wang, W. Wu and G. Wang, *Adv. Sci.*, 2019, **6**, 1900172.
164 S. K. Srivastava, G. Clergeaud, T. L. Andresen and A. Boisen, *Adv. Drug Delivery Rev.*, 2019, **138**, 41–55.
165 J. Loscalzo, *Circulation*, 2018, **137**, 233–236.
166 R. K. Richelsen, T. F. Overvad and S. E. Jensen, *J. Cardiol. Ther.*, 2016, **5**, 133–160.
167 X. Tang, L. Chen, Z. Wu, Y. Li, J. Zeng, W. Jiang, W. Lv, M. Wan, C. Mao and M. Zhou, *Small*, 2023, **19**, e2203238.
168 S. Chen, Y. Chen, M. Fu, Q. Cao, B. Wang, W. Chen and X. Ma, *J. Mater. Chem. B*, 2022, **10**, 7099–7107.
169 S. Liu, C. Gao and F. Peng, *Mater. Today Adv.*, 2022, **16**, 100281.
170 M. Ikram, F. Hu, G. Peng, M. Basharat, N. Jabeen, K. Pan and Y. Gao, *ACS Appl. Mater. Interfaces*, 2021, **13**, 51799–51806.
171 D. Zhou, R. Zhuang, X. Chang and L. Li, *Research*, 2020, **25**, 2639–5274.
172 J. Palacci, S. Sacanna, A. Vatchinsky, P. M. Chaikin and D. J. Pine, *J. Am. Chem. Soc.*, 2013, **135**, 15978–15981.
173 P. Nakielski, S. Pawłowska, C. Rinoldi, Y. Ziai, L. De Sio, O. Urbanek, K. Zembrzycki, M. Pruchniewski, M. Lanzi, E. Salatelli, A. Calogero, T. A. Kowalewski, A. L. Yarin and F. Pierini, *ACS Appl. Mater. Interfaces*, 2020, **12**, 54328–54342.
174 R. Dong, Y. Hu, Y. Wu, W. Gao, B. Ren, Q. Wang and Y. Cai, *J. Am. Chem. Soc.*, 2017, **139**, 1722–1725.
175 J. Li, P. S. Kollipara, Y. Liu, K. Yao, Y. Liu and Y. Zheng, *ACS Nano*, 2022, **16**, 8820–8826.
176 D. R. S. Pooler, A. S. Lubbe, S. Crespi and B. L. Feringa, *Chem. Sci.*, 2021, **12**, 14964–14986.
177 C. Chen, F. Mou, L. Xu, S. Wang, J. Guan, Z. Feng, Q. Wang, L. Kong, W. Li, J. Wang and Q. Zhang, *Adv. Mater.*, 2017, **29**, 1603374.
178 X. Guo, Y. Wang, F. Mou, Q. Xie, S. Su, C. Chen and J. Guan, *J. Mater. Chem. C*, 2022, **10**, 5079–5087.
179 L. Li, Z. Yu, J. Liu, M. Yang, G. Shi, Z. Feng, W. Luo, H. Ma, J. Guan and F. Mou, *Nano-Micro Lett.*, 2023, **15**, 2150–5551.
180 M. Yang, X. Guo, F. Mou and J. Guan, *Chem. Rev.*, 2023, **123**, 3944–3975.
181 A. Servant, F. Qiu, M. Mazza, K. Kostarelos and B. J. Nelson, *Adv. Mater.*, 2015, **27**, 2981–2988.
182 L. Zhu, D. Gao, L. Xie, Y. Dai and Q. Zhao, *Mol. Pharm.*, 2020, **17**, 3720–3729.
183 Y. Wang, W. Chen, Z. Wang, Y. Zhu, H. Zhao, K. Wu, J. Wu, W. Zhang, Q. Zhang, H. Guo, H. Ju and Y. Liu, *Angew. Chem., Int. Ed.*, 2023, **62**, e202212866.
184 R. Wu, Z. Yao, Z. Chen, X. Ge, L. Su, S. Wang, Y. Wu and J. Song, *Anal. Chem.*, 2023, **95**, 11219–11226.
185 D. Xue, Y. Wang and H. Zhang, *Adv. Opt. Mater.*, 2023, **11**, 2202888.
186 B. Hou, L. Yi, D. Hu, Z. Luo, D. Gao, C. Li, B. Xing, J.-W. Wang, C. N. Lee, R. Zhang, Z. Sheng, B. Zhou and X. Liu, *Nat. Biomed. Eng.*, 2023, **22**, 2157–2846X.
187 Y. Ran, Z. Xu, M. Chen, W. Wang, Y. Wu, J. Cai, J. Long, Z.-S. Chen, D. Zhang and B.-O. Guan, *Adv. Sci.*, 2022, **9**, 2200456.
188 H. Zhang, Z. Zhao, S. Sun, S. Zhang, Y. Wang, X. Zhang, J. Sun, Z. He, S. Zhang and C. Luo, *Nat. Commun.*, 2023, **14**, 255–268.
189 H. Wang, Y. Guo, C. Wang, X. Jiang, H. Liu, A. Yuan, J. Yan, Y. Hu and J. Wu, *Biomaterials*, 2021, **269**, 120621.
190 F. Scalambra, I. F. Díaz-Ortega and A. Romerosa, *Dalton Trans.*, 2022, **51**, 14022–14031.
191 S. Zhang, M. Li, J. Wang, Y. Zhou, P. Dai, M. Zhao, W. Lv, S. Liu and Q. Zhao, *Bioconjugate Chem.*, 2023, **34**, 1327–1335.

192 Y. Xu, H. Li, S. Xu, X. Liu, J. Lin, H. Chen and Z. Yuan, *J. Med. Chem.*, 2022, **65**, 424–435.
193 H. He, Y. Liu, Z. Zhou, C. Guo, H.-Y. Wang, Z. Wang, X. Wang, Z. Zhang, F.-G. Wu, H. Wang, D. Chen, D. Yang, X. Liang, J. Chen, S. Zhou, X. Liang, X. Qian and Y. Yang, *Free Radical Biol. Med.*, 2018, **123**, 1–7.
194 A. Sikder, R. Mengji, S. Mondal, A. Jana and N. D. P. Singh, *J. Mater. Chem. B*, 2023, **11**, 5131–5141.
195 R. D. Hurst and I. B. Fritz, *J. Cell. Physiol.*, 1996, **167**, 89–94.
196 T. Kim, H. J. Kim, W. Choi, Y. M. Lee, J. H. Pyo, J. Lee, J. Kim, J. Kim, J.-H. Kim, C. Kim and W. J. Kim, *Nat. Biomed. Eng.*, 2023, **7**, 149–163.
197 S. Li, R. Liao, X. Sheng, X. Luo, X. Zhang, X. Wen, J. Zhou and K. Peng, *Front. Oncol.*, 2019, **9**, 696.
198 S. M. Andrabi, N. S. Sharma, A. Karan, S. M. S. Shahriar, B. Cordon, B. Ma and J. Xie, *Adv. Sci.*, 2023, **10**, 2303259.
199 G. Cirino, C. Szabo and A. Papapetropoulos, *Physiol. Rev.*, 2023, **103**, 31–276.
200 S. Fu, D. Fu, D. Xie, L. Liu, B. Chen, Y. Ye, D. A. Wilson and F. Peng, *Appl. Mater. Today*, 2022, **26**, 101348.
201 J. Feng, S.-P. Yang, Y.-Q. Shao, Y.-Y. Sun, Z.-L. He, Y. Wang, Y.-N. Zhai and Y.-B. Dong, *Adv. Healthcare Mater.*, 2023, **12**, 2301645.
202 Z. Li, S. Fu, H. Li, B. Chen, D. Xie, D. Fu, Y. Feng, C. Gao, S. Liu, D. A. Wilson, Y. Tu and F. Peng, *Chem. Eng. J.*, 2023, **468**, 143393.
203 J.-M. Lehn, *Angew. Chem., Int. Ed. Engl.*, 1988, **27**, 89–112.
204 M. Liu, J. Jiang, H. Tan, B. Chen, J. Ou, H. Wang, J. Sun, L. Liu, F. Wang, J. Gao, C. Liu, F. Peng, Y. Liu and Y. Tu, *Nanoscale*, 2022, **14**, 12804–12813.
205 V. Sridhar, B. W. Park and M. Sitti, *Adv. Funct. Mater.*, 2018, **28**, 1704902.
206 Y. Xing, S. Tang, X. Du, T. Xu and X. Zhang, *Nano Res.*, 2020, **14**, 654–659.
207 Y. Wang, W. Chen, Z. Wang, Y. Zhu, H. Zhao, K. Wu, J. Wu, W. Zhang, Q. Zhang, H. Guo, H. Ju and Y. Liu, *Angew. Chem., Int. Ed.*, 2023, **62**, e202212866.
208 D. Wang, J. Jiang, B. Hao, M. Li, Z. Chen, H. Zhang, X. Wang and B. Dong, *Appl. Mater. Today*, 2022, **29**, 101652.
209 W. Liu, X. Chen, X. Ding, Q. Long, X. Lu, Q. Wang and Z. Gu, *Nanoscale Horiz.*, 2021, **6**, 238–244.
210 Z. Ni, D. Zhang, S. Zhen, X. Liang, X. Gong, Z. Zhao, D. Ding, G. Feng and B. Tang, *Biomaterials*, 2023, **301**, 122261.